J. Plasma Phys. (2023), *vol*. 89, 905890604
Published by Cambridge University Press

doi:10.1017/S002237782300123X

Generalized cross-helicity in non-ideal magnetohydrodynamics

Prachi Sharma [1] **and Asher Yahalom** [1,†]

[1] Ariel University, Kiryat Hamada POB 3, Ariel 40700, Israel

(Received 9 April 2023; revised 29 October 2023; accepted 8 November 2023)

The objective of the present paper is to investigate the constancy of the topological invariant, denoted the non-barotropic generalized cross-helicity in the case of non-ideal magnetohydrodynamics (MHD). Existing work considers only ideal barotropic MHD and ideal non-barotropic MHD. Here, we consider dissipative processes in the form of thermal conduction, finite electrical conductivity and viscosity and the effect of these processes on the cross-helicity conservation. An analytical approach has been adopted to obtain the mathematical expressions for the time derivative of the cross-helicity. Obtained results show that the generalized cross-helicity is not conserved in the non-ideal MHD limit and indicate which processes affect the helicity and which do not. Furthermore, we indicate the configurations in which this topological constant is conserved despite the dissipative processes. Some examples and applications are also given.

Keywords: plasma flows

1. Introduction

Topological invariants have been useful for several decades, and there are such invariants in magnetohydrodynamic (MHD) flows. For example, the importance of two helicities i.e. magnetic helicity and cross-helicity, has long been discussed in relation to the controlled nuclear fusion problem and in numerous astrophysical scenarios (Brown *et al.* 1999; Yoshizawa & Yokoi 1993; Yoshizawa 1991; Vishniac & Cho 2001 and references therein). Earlier works (Yahalom & Lynden-Bell 2008; Yahalom 2013, 1995) have studied the relations between the helicities and symmetries of ideal MHD. Magnetohydrodynamics connects Maxwell's equations to the hydrodynamics of highly conductive flows to explain the macroscopic behaviour of a conducting fluid such as a plasma. The simplest fluid model to explain the characteristics of a plasma is ideal MHD. Ideal MHD is characterized by an infinite electrical conductivity or, alternatively, by the limit at which electrical resistivity disappears. In this case, the magnetic field is frozen in the plasma and no topological modifications are conceivable. Freidberg (1987) has discussed the role of ideal MHD in the regime of plasma physics. However, ideal MHD does not describe precisely the behaviour of real plasmas and this is the main motivation

† Email address for correspondence: asya@ariel.ac.il

for the study of non-ideal MHD. Some important realistic processes are missing in the ideal description, such as resistive heating, heat conduction and viscous effects. Viscosity plays an important role on the dissipation scale when investigating plasma turbulence in the solar wind and elsewhere. Similarly, magnetic diffusivity is one of the reasons for the magnetic reconnection phenomenon. Thermal conductivity is also a substantial process in more realistic models (Landau & Lifshitz 1987). It causes the perturbations of the physical variables to spread out through a plasma. These essential properties of all three dissipative processes are the stimuli for the authors to make this current analysis.

The mathematical expression for cross-helicity (correlation between the velocity and magnetic field) is given by (Woltjer 1958*b*,*a*)

$$H_C = \int \boldsymbol{B} \cdot \boldsymbol{v} \, \mathrm{d}^3 x, \tag{1.1}$$

in which the integral is taken over the entire flow domain. Here, $\boldsymbol{B}$ and $\boldsymbol{v}$ are the magnetic field and velocity, respectively; H_C is conserved for barotropic or incompressible MHD (but not for non-barotropic MHD) and is given a topological interpretation in terms of the knottiness of the magnetic and flow field lines. A generalization for non-barotropic MHD of this quantity was given by Webb *et al.* (2014*a*,*b*). This resembles the generalization of barotropic fluid dynamics conserved quantities including helicity to non-barotropic flows, including topological constants of motion derived by Mobbs (1981). The conservation law of cross-helicity for non-barotropic MHD has been discussed by Webb, McKenzie & Zank (2015) in a multi-symplectic formulation of MHD. A potential vorticity conservation equation for non-barotropic MHD was derived by Webb & Mace (2015) by using Noether's second theorem. Webb *et al.* (2014*a*,*b*) pointed out that the generalized helicity conservation law in non-barotropic fluids is not local, as it relies on the extra, non-locally generated variable σ, which is derived from the Lagrangian time integral of the temperature $T(x, t)$. Here, $\boldsymbol{v}$ is replaced by the topological velocity field $\boldsymbol{v}_t = \boldsymbol{v} - \sigma \nabla s$. The mathematical expression of non-barotropic cross-helicity is given in section 3.

Recently, the non-barotropic cross-helicity was generalized using additional label translation symmetry groups (χ and η translations) (Yahalom 2019), this led to additional topological conservation laws, the χ and η cross-helicities. The functions χ and η are sometimes denoted as 'Euler potentials', 'Clebsch variables' and also 'flux representation functions' (Hazeltine & Meiss 2003).

Cross-helicity is expected to play an important role in several MHD plasma phenomena such as global magnetic field generation, turbulence suppression, etc. It provides a measure of the degree of linkage of the vortex tubes of the velocity field with the flux tubes of the magnetic field. Cross-helicity plays an important role in the turbulent dynamo (Yokoi 2013). The cross-helicity density conservation law for barotropic flows is important in MHD turbulence theory (Zhou & Matthaeus 1990*b*,*a*; Zank *et al.* 2011). Verma (2004) has discussed MHD turbulence in his review paper in detail. He has examined Alfvénic MHD turbulence with zero and non-zero helicities. Plasma velocity and magnetic field measurements from the Voyager 2 mission are used to study solar wind turbulence in the slow solar wind (Iovieno *et al.* 2016) and to characterize its cross-helicity. The energy fluxes of MHD turbulence provide a measure for the transfers of energy among the velocity and magnetic fields (Verma 2019; Verma *et al.* 2021).

Magnetic helicity that characterizes the topological features of magnetic field lines (Woltjer 1958*b*; Moffatt 1969, 1978; Moffatt & Ricca 1995; Webb *et al.* 2014*a*,*b*) is given

https://doi.org/10.1017/S002237782300123X Published online by Cambridge University Press

by

$$H_M \equiv \int \boldsymbol{A} \cdot \boldsymbol{B} \, \mathrm{d}^3 x. \tag{1.2}$$

Calkin (1963) and Webb & Anco (2017) used gauge field theory to obtain the conservation law for the magnetic helicity density for ideal MHD. Here, $\boldsymbol{A}$ is the vector potential. Faraco & Lindberg (2020) has also shown the conservation of magnetic helicity in turbulent flows. Barnes *et al.* (1986) showed the dissipation of the magnetic field when flux tubes diffuse through one another on resistive time scales. Candelaresi & Del Sordo (2021) show that helical magnetic fields play a major role in ensuring the sustained stability of some plasmas, based on their observational, numerical and analytical results. Further, its important role in determining the structures, dynamics and heating of the solar corona has been well explained by Knizhnik *et al.* (2019).

The present work is the first treatment of the evolution of generalized cross-helicity considering dissipative processes. In addition to the general presented result of non-barotropic cross-helicity dissipation by friction, magnetic diffusivity and heat conduction, we also give a specific analytic model of MHD with finite diffusivity and compare the decay of cross-helicity with the decay of magnetic helicity for the case of high magnetic Reynolds number.

The structure of this paper is as follows: the second section deals with the basic equations for non-ideal non-barotropic MHD and defines the basic notations. In the section that follows, we introduce non-barotropic cross-helicity and show how it decays under non-ideal processes. We conclude the third section by comparing this decay with the decay of magnetic helicity. Section four describes the decay in a framework of a simple but completely analytic model. Section five discuss the constraints imposed by topological quantities on the MHD dynamics. Section six is concerned with the effect of cross-helicity on the Z pinch. Section seven concludes the current paper with some general remarks and plans for future developments.

2. Standard formulation of non-ideal non-barotropic MHD

The standard set of equations solved for non-ideal non-barotropic MHD is given below (here. we use the EMU system of units)

$$\begin{aligned}\rho \frac{\mathrm{d}\boldsymbol{v}}{\mathrm{d}t} &= \rho \left[\frac{\partial \boldsymbol{v}}{\partial t} + (\boldsymbol{v} \cdot \nabla)\boldsymbol{v} \right] = -\nabla p + \boldsymbol{J} \times \boldsymbol{B} - \rho \nabla \phi + \frac{\partial \sigma'_{ik}}{\partial x_k} \\ &= -\nabla p + \frac{(\nabla \times \boldsymbol{B}) \times \boldsymbol{B}}{4\pi} - \rho \nabla \phi + \frac{\partial \sigma'_{ik}}{\partial x_k},\end{aligned} \tag{2.1}$$

$$\frac{\partial \rho}{\partial t} + \nabla \cdot (\rho \boldsymbol{v}) = 0 \tag{2.2}$$

$$\nabla \cdot \boldsymbol{B} = 0 \tag{2.3}$$

$$\frac{\partial \boldsymbol{B}}{\partial t} = \nabla \times (\boldsymbol{v} \times \boldsymbol{B}) + \frac{\eta}{4\pi} \nabla^2 \boldsymbol{B} \tag{2.4}$$

$$\rho T \frac{\mathrm{d}s}{\mathrm{d}t} = \sigma'_{ik} \frac{\partial v_i}{\partial x_k} + \eta J^2 + \nabla \cdot (k \nabla T). \tag{2.5}$$

The following notations are utilized: $\partial/\partial t$ is the partial temporal derivative; $\mathrm{d}/\mathrm{d}t = \partial/\partial t + \boldsymbol{v} \cdot \nabla$ is the temporal material derivative or Lagrangian time derivative; ∇ has

https://doi.org/10.1017/S002237782300123X Published online by Cambridge University Press

its standard meaning in vector calculus; ρ is the fluid density, $\boldsymbol{v}$ is the velocity of fluid, $\boldsymbol{B}$ is the magnetic flux density, ϕ is a gravitational potential, T is the temperature, s is the specific entropy, k is the heat conduction and p is the pressure, which depends through the equation of state on the density and entropy (the non-barotropic case). The stress tensor is defined as

$$\sigma'_{ik} = \mu\left(\frac{\partial v_i}{\partial x_k} + \frac{\partial v_k}{\partial x_i} - \frac{2}{3}\delta_{ik}\frac{\partial v_l}{\partial x_l}\right), \tag{2.6}$$

in which μ is a coefficient of kinematic viscosity. Notice that we take the coefficient of second viscosity (or volume viscosity) to be zero for the sake of simplicity. According to classical kinetic theory, viscosity arises from collisions between particles. The current density $\boldsymbol{J}$ and the magnetic field are related by Ampere's law (EMU units)

$$\nabla \times \boldsymbol{B} = 4\pi \boldsymbol{J}. \tag{2.7}$$

Note that Maxwell's displacement current is often neglected due to its smallness in MHD dynamics in the non-relativistic regime. The magnetic diffusivity η originates from Ohm's law

$$\boldsymbol{E} + \boldsymbol{v} \times \boldsymbol{B} = \eta \boldsymbol{J}, \tag{2.8}$$

of non-ideal MHD, where $\boldsymbol{E}$ is the electric field. Ohm's law is another manifestation of collisions in the plasma. Combining Ohm's equation with Faraday's equation

$$\frac{\partial \boldsymbol{B}}{\partial t} = -\nabla \times \boldsymbol{E}, \tag{2.9}$$

and Ampere's law will yield (2.4). In this form, η resembles a diffusion coefficient describing the diffusion of the magnetic field through a conducting medium of finite conductivity. The justification for those equations and the conditions under which they apply can be found in standard books on MHD (see for e.g. Batchelor 1967; Landau & Lifshitz 1987; Sturrock 1994; Kundu, Cohen & Dowling 2015; Ogilvie 2016).

3. Cross-helicity for non-ideal non-barotropic MHD

In this section, we derive the time derivative of the non-barotropic cross-helicity using the aforementioned equations.

3.1. *A brief explanation of the topological velocity and non-barotropic cross-helicity*

The mathematical expression for the cross-helicity of non-barotropic fluids is given by (Webb *et al.* 2014*a*; Yahalom 2017*a*,*b*)

$$H_{CNB} = \int \mathrm{d}^3x\, \boldsymbol{v}_t \cdot \boldsymbol{B}. \tag{3.1}$$

Here, the topological velocity field is defined as $\boldsymbol{v_t} = \boldsymbol{v} - \sigma\nabla s$ (Yahalom & Qin 2021), where σ is an auxiliary variable, which depends on the Lagrangian time integral of the temperature i.e.

$$\frac{\mathrm{d}\sigma}{\mathrm{d}t} = T. \quad \left(\Rightarrow \sigma = \int_0^t T\,\mathrm{d}t' + \sigma_0 = t\langle T\rangle + \sigma_0\right). \tag{3.2}$$

The above integral is done for each fluid element separately and $\langle\rangle = (1/t)\int_0^t \mathrm{d}t'$ designates temporal averaging. In Appendix A we describe the variational approach leading to (3.2).

https://doi.org/10.1017/S002237782300123X Published online by Cambridge University Press

Notice that, in non-barotropic MHD, one can calculate the temporal derivative of the cross-helicity equation (1.1) using the standard equations to obtain

$$\frac{\mathrm{d}H_C}{\mathrm{d}t} = \int T\nabla s \cdot \boldsymbol{B}\, \mathrm{d}^3x. \tag{3.3}$$

Thus, generically, cross-helicity is not conserved. A clue on how to define the cross-helicity for non-barotropic MHD can be obtained from the variational analysis described in Yahalom (2016*b*), which is valid for magnetic field lines at the intersection of two comoving surfaces χ, η_0 (Euler potentials). Following Sakurai (1979), the magnetic field takes the form

$$\boldsymbol{B} = \nabla\chi \times \nabla\eta_0. \tag{3.4}$$

And the generalized Clebsch representation of the velocity (Yahalom 2016*b*) is

$$\boldsymbol{v} = \nabla\nu + \alpha\nabla\chi + \beta\nabla\eta_0 + \sigma\nabla s, \tag{3.5}$$

where, in the above, α, β and ν are Lagrange multipliers appearing in the said action (Yahalom 2016*b*); see also Appendix A. Let us now write the cross-helicity given in (1.1) in terms of (3.4) and (3.5), this will take the form

$$H_C = \int \mathrm{d}\Phi[\nu] + \int \mathrm{d}\Phi \oint \sigma\, \mathrm{d}s, \tag{3.6}$$

in which $\mathrm{d}\Phi = \boldsymbol{B} \cdot \mathrm{d}\boldsymbol{S}$ is the magnetic flux, and $[\nu]$ is the discontinuity of the non-single valued potential ν (Yahalom 2017*a*). Now, as for ideal MHD, the magnetic field lines move with the flow, and it follows that the magnetic flux $\mathrm{d}\Phi$ is conserved. It is also shown in Yahalom (2017*a*) that the material derivative of $[\nu]$ must vanish. Thus, the first term on the right-hand side of (3.6) is conserved. This suggests the following definition for the non-barotropic cross-helicity H_{CNB}

$$H_{CNB} = \int \mathrm{d}\Phi[\nu] = H_C - \int \mathrm{d}\Phi \oint \sigma\, \mathrm{d}s. \tag{3.7}$$

The conventional form of the same expression is given in (3.1). Please refer to Yahalom (2017*a*) for the detailed justification of the definition, the form of the non-barotropic cross-helicity and a proof of its constancy.

We point out that, from a pure mathematical point of view, it does not really matter what the physical meaning of the vector fields appearing in the cross-helicity term is, the cross-helicity will describe how the fields are knotted together (Yokoi 2013, § 2, see also Ricca & Moffatt (1992) and Ricca & Berger (1996) for non-crossed helicity). Thus, from a purely topological point of view, it does not matter if we consider the physical velocity field $\boldsymbol{v}$ or the topological velocity field $\boldsymbol{v}_t$.

3.2. *The temporal derivative of non-barotropic cross-helicity*

Next, we study the temporal derivative of the non-barotropic cross-helicity

$$\frac{\mathrm{d}H_{CNB}}{\mathrm{d}t} = \int \mathrm{d}^3x \left(\boldsymbol{v}_t \cdot \frac{\partial \boldsymbol{B}}{\partial t} + \boldsymbol{B} \cdot \frac{\partial \boldsymbol{v}_t}{\partial t}\right). \tag{3.8}$$

https://doi.org/10.1017/S002237782300123X Published online by Cambridge University Press

Now we calculate the first term on the right-hand side with the help of (2.4)

$$\boldsymbol{v}_t \boldsymbol{\cdot} \frac{\partial \boldsymbol{B}}{\partial t} = \boldsymbol{v}_t \boldsymbol{\cdot} \left\{\nabla \times (\boldsymbol{v} \times \boldsymbol{B}) + \frac{\eta}{4\pi}\nabla^2 \boldsymbol{B}\right\} \tag{3.9}$$

$$\boldsymbol{v}_t \boldsymbol{\cdot} \frac{\partial \boldsymbol{B}}{\partial t} = \nabla \boldsymbol{\cdot} \{(\boldsymbol{v} \times \boldsymbol{B}) \times \boldsymbol{v}_t\} + (\boldsymbol{v} \times \boldsymbol{B}) \boldsymbol{\cdot} \boldsymbol{\omega}_t + \boldsymbol{v}_t \boldsymbol{\cdot} \frac{\eta}{4\pi}\nabla^2 \boldsymbol{B}, \tag{3.10}$$

where we define the topological vorticity of the topological flow field as

$$\boldsymbol{\omega}_t \equiv \nabla \times \boldsymbol{v}_t. \tag{3.11}$$

Next, we calculate the second term on the right-hand side

$$\boldsymbol{B} \boldsymbol{\cdot} \frac{\partial \boldsymbol{v}_t}{\partial t} = \boldsymbol{B} \boldsymbol{\cdot} \frac{\partial(\boldsymbol{v} - \sigma\nabla s)}{\partial t} = \boldsymbol{B} \boldsymbol{\cdot} \left(\frac{\partial \boldsymbol{v}}{\partial t} - \frac{\partial \sigma}{\partial t}\nabla s - \sigma\nabla\frac{\partial s}{\partial t}\right). \tag{3.12}$$

Now we simplify the right-hand side of (3.12) in three steps: the first term is calculated with the help of (2.1)

$$\begin{aligned}\frac{\partial \boldsymbol{v}}{\partial t} &= -(\boldsymbol{v} \boldsymbol{\cdot} \nabla)\boldsymbol{v} - \frac{\nabla p}{\rho} + \frac{(\nabla \times \boldsymbol{B}) \times \boldsymbol{B}}{4\pi\rho} - \nabla\phi + \frac{1}{\rho}\frac{\partial \sigma'_{ik}}{\partial x_k} \\ &= (\boldsymbol{v} \times \boldsymbol{\omega}) + \frac{(\nabla \times \boldsymbol{B}) \times \boldsymbol{B}}{4\pi\rho} - \nabla\left(\frac{v^2}{2}\right) - \nabla w + T\nabla s - \nabla\phi + \frac{1}{\rho}\frac{\partial \sigma'_{ik}}{\partial x_k},\end{aligned} \tag{3.13}$$

in which the vorticity is

$$\boldsymbol{\omega} \equiv \nabla \times \boldsymbol{v}, \tag{3.14}$$

and we have used the thermodynamic identity

$$\mathrm{d}w = \mathrm{d}\varepsilon + \mathrm{d}\left(\frac{p}{\rho}\right) = T\,\mathrm{d}s + \frac{1}{\rho}\mathrm{d}p \Rightarrow \nabla w = T\nabla s + \frac{1}{\rho}\nabla p. \tag{3.15}$$

Thus

$$\boldsymbol{B} \boldsymbol{\cdot} \frac{\partial \boldsymbol{v}}{\partial t} = \boldsymbol{B} \boldsymbol{\cdot} \left\{(\boldsymbol{v} \times \boldsymbol{\omega}) - \nabla\left(\frac{v^2}{2} + w + \phi\right) + T\nabla s\right\} + \frac{B_i}{\rho}\frac{\partial \sigma'_{ik}}{\partial x_k}. \tag{3.16}$$

In the second term, we use (3.2) to obtain

$$-\frac{\partial \sigma}{\partial t}\nabla s = (\boldsymbol{v} \boldsymbol{\cdot} \nabla\sigma - T)\nabla s. \tag{3.17}$$

In the third term, we use (2.5) to derive

$$-\sigma\nabla\frac{\partial s}{\partial t} = \sigma\nabla\left[\boldsymbol{v} \boldsymbol{\cdot} \nabla s - \frac{1}{\rho T}\sigma'_{ik}\frac{\partial v_i}{\partial x_k} - \frac{\eta}{\rho T}J^2 - \frac{1}{\rho T}\nabla \boldsymbol{\cdot} (k\nabla T)\right]. \tag{3.18}$$

Combining the above expressions, we have

$$\begin{aligned}\boldsymbol{B} \boldsymbol{\cdot} \frac{\partial \boldsymbol{v}_t}{\partial t} = \boldsymbol{B} \boldsymbol{\cdot} \Bigg[&(\boldsymbol{v} \times \boldsymbol{\omega}) - \nabla\left(\frac{v^2}{2} + w + \phi\right) + (\boldsymbol{v} \boldsymbol{\cdot} \nabla\sigma)\nabla s + \sigma\nabla(\boldsymbol{v} \boldsymbol{\cdot} \nabla s) \\ &+ \sigma\nabla\left\{-\frac{1}{\rho T}\sigma'_{ik}\frac{\partial v_i}{\partial x_k} - \frac{\eta}{\rho T}J^2 - \frac{1}{\rho T}\nabla \boldsymbol{\cdot} (k\nabla T)\right\}\Bigg] + \frac{B_i}{\rho}\frac{\partial \sigma'_{ik}}{\partial x_k}.\end{aligned} \tag{3.19}$$

https://doi.org/10.1017/S002237782300123X Published online by Cambridge University Press

Notice that

$$\nabla\{\sigma(\boldsymbol{v}\cdot\nabla s)\}=\sigma\nabla(\boldsymbol{v}\cdot\nabla s)+(\boldsymbol{v}\cdot\nabla s)\nabla\sigma, \tag{3.20}$$

and also that

$$\begin{aligned}\boldsymbol{v}\times\boldsymbol{\omega}_t=\boldsymbol{v}\times(\boldsymbol{\omega}-\nabla\sigma\times\nabla s)&=\boldsymbol{v}\times\boldsymbol{\omega}+(\boldsymbol{v}\cdot\nabla\sigma)\nabla s-(\boldsymbol{v}\cdot\nabla s)\nabla\sigma\\ &=\boldsymbol{v}\times\boldsymbol{\omega}+(\boldsymbol{v}\cdot\nabla\sigma)\nabla s-\nabla((\boldsymbol{v}\cdot\nabla s)\sigma)+\sigma\nabla(\boldsymbol{v}\cdot\nabla s),\end{aligned} \tag{3.21}$$

or that

$$\boldsymbol{v}\times\boldsymbol{\omega}_t+\nabla((\boldsymbol{v}\cdot\nabla s)\sigma)=\boldsymbol{v}\times\boldsymbol{\omega}+(\boldsymbol{v}\cdot\nabla\sigma)\nabla s+\sigma\nabla(\boldsymbol{v}\cdot\nabla s). \tag{3.22}$$

Thus we obtain

$$\begin{aligned}\boldsymbol{B}\cdot\frac{\partial\boldsymbol{v}_t}{\partial t}&=\boldsymbol{B}\cdot\left[(\boldsymbol{v}\times\boldsymbol{\omega}_t)+\nabla\left\{\sigma(\boldsymbol{v}\cdot\nabla s)-\frac{v^2}{2}-w-\phi\right\}\right]\\ &\quad-\boldsymbol{B}\cdot\left[\sigma\nabla\left\{\frac{1}{\rho T}\sigma'_{ik}\frac{\partial v_i}{\partial x_k}+\frac{\eta}{\rho T}J^2+\frac{1}{\rho T}\nabla\cdot(k\nabla T)\right\}\right]+\frac{B_i}{\rho}\frac{\partial\sigma'_{ik}}{\partial x_k}.\end{aligned} \tag{3.23}$$

Combining (3.10) and (3.23) and taking into account that

$$\boldsymbol{B}\cdot(\boldsymbol{v}\times\boldsymbol{\omega}_t)=-(\boldsymbol{v}\times\boldsymbol{B})\cdot\boldsymbol{\omega}_t, \tag{3.24}$$

we obtain

$$\begin{aligned}\boldsymbol{v}_t\cdot\frac{\partial\boldsymbol{B}}{\partial t}+\frac{\partial\boldsymbol{v}_t}{\partial t}\cdot\boldsymbol{B}&=\nabla\cdot\{(\boldsymbol{v}\times\boldsymbol{B})\times\boldsymbol{v}_t\}+\frac{\eta}{4\pi}\boldsymbol{v}_t\cdot\nabla^2\boldsymbol{B}\\ &\quad+\boldsymbol{B}\cdot\nabla\left\{\sigma(\boldsymbol{v}\cdot\nabla s)-\frac{v^2}{2}-w-\phi\right\}\\ &\quad+\frac{B_i}{\rho}\frac{\partial\sigma'_{ik}}{\partial x_k}-\sigma\boldsymbol{B}\cdot\nabla\left\{\frac{1}{\rho T}\sigma'_{ik}\frac{\partial v_i}{\partial x_k}+\frac{\eta}{\rho T}J^2+\frac{k}{\rho T}\nabla^2 T\right\}\\ &=\nabla\cdot\left[\{(\boldsymbol{v}\times\boldsymbol{B})\times\boldsymbol{v}_t\}+\boldsymbol{B}\left\{\sigma(\boldsymbol{v}\cdot\nabla s)-\frac{v^2}{2}-w-\phi\right\}\right.\\ &\quad\left.-\sigma\boldsymbol{B}\left\{\frac{1}{\rho T}\sigma'_{ik}\frac{\partial v_i}{\partial x_k}+\frac{\eta}{\rho T}J^2+\frac{k}{\rho T}\nabla^2 T\right\}\right]\\ &\quad+\frac{\eta}{4\pi}\boldsymbol{v}_t\cdot\nabla^2\boldsymbol{B}+\frac{B_i}{\rho}\frac{\partial\sigma'_{ik}}{\partial x_k}\\ &\quad+(\boldsymbol{B}\cdot\nabla\sigma)\left[\frac{1}{\rho T}\sigma'_{ik}\frac{\partial v_i}{\partial x_k}+\frac{\eta}{\rho T}J^2+\frac{k}{\rho T}\nabla^2 T\right].\end{aligned} \tag{3.25}$$

https://doi.org/10.1017/S002237782300123X Published online by Cambridge University Press

Now, substituting (3.25) into (3.8), we obtain

$$\begin{aligned}\frac{\mathrm{d}H_{\mathrm{CNB}}}{\mathrm{d}t} &= \int \nabla \cdot \left[\{(\boldsymbol{v} \times \boldsymbol{B}) \times \boldsymbol{v}_t\} + \boldsymbol{B} \left\{ \sigma (\boldsymbol{v} \cdot \nabla s) - \frac{v^2}{2} - w - \phi \right\} \right. \\ &\quad \left. - \sigma \boldsymbol{B} \left\{ \frac{1}{\rho T} \sigma'_{ik} \frac{\partial v_i}{\partial x_k} + \frac{\eta}{\rho T} J^2 + \frac{k}{\rho T} \nabla^2 T \right\} \right] \mathrm{d}^3 x \\ &\quad + \int \left\{ \frac{\eta}{4\pi} \boldsymbol{v}_t \cdot \nabla^2 \boldsymbol{B} + \frac{B_i}{\rho} \frac{\partial \sigma'_{ik}}{\partial x_k} \right. \\ &\quad \left. + (\boldsymbol{B} \cdot \nabla \sigma) \left[\frac{1}{\rho T} \sigma'_{ik} \frac{\partial v_i}{\partial x_k} + \frac{\eta}{\rho T} J^2 + \frac{k}{\rho T} \nabla^2 T \right] \right\} \mathrm{d}^3 x, \end{aligned} \tag{3.26}$$

using Gauss' divergence theorem, we obtain

$$\begin{aligned}\frac{\mathrm{d}H_{\mathrm{CNB}}}{\mathrm{d}t} &= \oint \left[\{(\boldsymbol{v} \times \boldsymbol{B}) \times \boldsymbol{v}_t\} + \boldsymbol{B} \left\{ \sigma (\boldsymbol{v} \cdot \nabla s) - \frac{v^2}{2} - w - \phi \right\} \right. \\ &\quad \left. - \sigma \boldsymbol{B} \left\{ \frac{1}{\rho T} \sigma'_{ik} \frac{\partial v_i}{\partial x_k} + \frac{\eta}{\rho T} J^2 + \frac{k}{\rho T} \nabla^2 T \right\} \right] \cdot \mathrm{d}\boldsymbol{S} \\ &\quad + \int \left\{ \frac{\eta}{4\pi} \boldsymbol{v}_t \cdot \nabla^2 \boldsymbol{B} + \frac{B_i}{\rho} \frac{\partial \sigma'_{ik}}{\partial x_k} \right. \\ &\quad \left. + (\boldsymbol{B} \cdot \nabla \sigma) \left[\frac{1}{\rho T} \sigma'_{ik} \frac{\partial v_i}{\partial x_k} + \frac{\eta}{\rho T} J^2 + \frac{k}{\rho T} \nabla^2 T \right] \right\} \mathrm{d}^3 x. \end{aligned} \tag{3.27}$$

Here, the surface integral encapsulates the volume for which the cross-helicity is calculated. For generic problems arising in the solar and dynamo contexts, the volume chosen is not infinite. Experience with magnetic helicity variation shows that the boundary terms are often critical (and the largest in the solar corona), and the topology flowing in and out of systems is crucial in astrophysical contexts. It would likely be so for the non-barotropic cross-helicity. If the surface is taken at infinity the magnetic fields vanish and thus, in a generic case, the entire surface term, then the time derivative of cross-helicity can be written as

$$\frac{\mathrm{d}H_{\mathrm{CNB}}}{\mathrm{d}t} = \int \left\{ \frac{\eta}{4\pi} \boldsymbol{v}_t \cdot \nabla^2 \boldsymbol{B} + \frac{B_i}{\rho} \frac{\partial \sigma'_{ik}}{\partial x_k} + \frac{(\boldsymbol{B} \cdot \nabla \sigma)}{\rho T} \left(\sigma'_{ik} \frac{\partial v_i}{\partial x_k} + \eta J^2 + k \nabla^2 T \right) \right\} \mathrm{d}^3 x. \tag{3.28}$$

Thus, the time derivative of the cross-helicity depends generically on the stress tensor i.e. the viscosity of the fluid and the coefficient of magnetic diffusivity, and also on the heat conduction but not on heat convection. By putting all non-ideal terms to zero, we obtain the ideal MHD condition and conservation of non-barotropic cross-helicity takes place. In the special case that the magnetic field lies on σ surfaces (that is, average temperature surfaces) and thus is orthogonal to $\nabla \sigma$, the cross-helicity change will not depend on the thermal conductivity

$$\frac{\mathrm{d}H_{\mathrm{CNB}}}{\mathrm{d}t} = \int \left\{ \frac{\eta}{4\pi} \boldsymbol{v}_t \cdot \nabla^2 \boldsymbol{B} + \frac{B_i}{\rho} \frac{\partial \sigma'_{ik}}{\partial x_k} \right\} \mathrm{d}^3 x. \tag{3.29}$$

The same will be true for a high density and high temperature plasma, and a plasma of small temperature gradients (plasma in global thermal equilibrium). Of course, even if heat conduction does not affect the non-barotropic cross-helicity, other non-ideal processes do, and those include friction and ohmic losses.

To conclude this subsection we shall partition the time derivative of the non-barotropic cross-helicity in accordance with the non-ideal process that contributes to its modification

$$\frac{\mathrm{d}H_{CNB}}{\mathrm{d}t} = \int \left\{ \eta \left[\frac{\boldsymbol{v}_t \boldsymbol{\cdot} \nabla^2 \boldsymbol{B}}{4\pi} + \frac{J^2}{\rho T}(\boldsymbol{B} \boldsymbol{\cdot} \nabla\sigma) \right] + k(\boldsymbol{B} \boldsymbol{\cdot} \nabla\sigma)\frac{\nabla^2 T}{\rho T} + \frac{B_i}{\rho}\frac{\partial \sigma'_{ik}}{\partial x_k} + (\boldsymbol{B} \boldsymbol{\cdot} \nabla\sigma)\frac{\sigma'_{ik}}{\rho T}\frac{\partial v_i}{\partial x_k} \right\} \mathrm{d}^3 x. \tag{3.30}$$

Let us introduce the dimensionless Reynolds number and magnetic Reynolds number

$$R_e \equiv \frac{\bar{\rho} U L}{\mu}, \quad R_m \equiv \frac{UL}{\eta}, \tag{3.31a,b}$$

where L is a characteristic length, $\bar{\rho}$ is a typical density and U a characteristic speed of the system.

We may now inquire: How does the value of those numbers affect the conservation of non-barotropic cross-helicity? To do this, we write each physical variable g as a multiplication of a characteristic value $\bar{g}$ and a dimensionless variable g' in the form

$$g = \bar{g} g' \quad \Rightarrow \quad \boldsymbol{x} = L\boldsymbol{x}', \quad \boldsymbol{v} = U\boldsymbol{v}', \quad t = \bar{t} t'. \tag{3.32a–c}$$

The above equation suggests the following choice of $\bar{t}$:

$$\bar{t} \equiv \frac{L}{U}. \tag{3.33}$$

Similarly, we write

$$\rho = \bar{\rho}\rho', \quad T = \bar{T}T', \quad \sigma = \bar{\sigma}\sigma', \quad \boldsymbol{B} = \bar{B}\boldsymbol{B}', \quad \boldsymbol{J} = \bar{J}\boldsymbol{J}'. \tag{3.34a–e}$$

Equation (3.2) suggests the following definition of $\bar{\sigma}$:

$$\bar{\sigma} \equiv \bar{T}\,\bar{t} = \frac{\bar{T}L}{U}, \tag{3.35}$$

and (2.7) suggests the following definition of $\bar{J}$:

$$\bar{J} \equiv \frac{\bar{B}}{L}. \tag{3.36}$$

For the viscosity tensor, we use a double prime notation (as we already used a single prime notation to distinguish the viscosity tensor from the σ scalar). Thus

$$\sigma'_{ik} = \bar{\sigma}'\sigma''_{ik}, \quad \sigma''_{ik} \equiv \frac{\partial v'_i}{\partial x'_k} + \frac{\partial v'_k}{\partial x'_i} - \frac{2}{3}\delta_{ik}\frac{\partial v'_l}{\partial x'_l}. \tag{3.37a,b}$$

It follows from (2.6) that

$$\bar{\sigma}' = \frac{\mu U}{L} = \frac{\bar{\rho} U^2}{R_e}. \tag{3.38}$$

https://doi.org/10.1017/S002237782300123X Published online by Cambridge University Press

We will also need the magnetic and kinetic energy expressions in dimensionless form

$$\left.\begin{aligned} E_k &= \frac{1}{2}\int \rho \boldsymbol{v}^2\,\mathrm{d}^3x = \bar{\rho}U^2L^3E'_k, \quad E'_k \equiv \frac{1}{2}\int \rho' \boldsymbol{v}'^2\,\mathrm{d}^3x' \\ E_m &= \frac{1}{8\pi}\int \boldsymbol{B}^2\,\mathrm{d}^3x = \bar{B}^2L^3E'_m, \quad E'_m \equiv \frac{1}{8\pi}\int \boldsymbol{B}'^2\,\mathrm{d}^3x'. \end{aligned}\right\} \tag{3.39}$$

Finally, we shall look at the amount of heat Q_c that is conducted into the volume (which is not equal to the total change in heat in the volume as heat may be produced by viscosity and ohmic losses; see (2.5)). We may write the heat flux density as

$$\boldsymbol{q} = \bar{q}\boldsymbol{q}', \quad \boldsymbol{q}' \equiv \boldsymbol{\nabla}'T', \quad \bar{q} \equiv k\frac{\bar{T}}{L}. \tag{3.40a–c}$$

Thus the rate of change of Q_c is (in dimensional and dimensionless form)

$$\frac{\mathrm{d}Q_c}{\mathrm{d}t} = -\oint \boldsymbol{q}\boldsymbol{\cdot}\mathrm{d}\boldsymbol{S} = -L^2\bar{q}\oint \boldsymbol{q}'\boldsymbol{\cdot}\mathrm{d}\boldsymbol{S}', \quad \frac{\mathrm{d}Q'_c}{\mathrm{d}t'} = -\oint \boldsymbol{q}'\boldsymbol{\cdot}\mathrm{d}\boldsymbol{S}', \tag{3.41a,b}$$

where we integrate over a surface encapsulating the flow. Writing as usual

$$\bar{Q}_c = \frac{Q_c}{Q'_c} = \bar{q}\frac{L^3}{U} = k\bar{T}\frac{L^2}{U}. \tag{3.42}$$

Having defined the above quantities, we may write the non-barotropic cross-helicity as

$$H_{\mathrm{CNB}} = \bar{H}_{\mathrm{CNB}}H'_{\mathrm{CNB}}, \quad \bar{H}_{\mathrm{CNB}} \equiv L^3U\bar{B}, \quad H'_{\mathrm{CNB}} \equiv \int \mathrm{d}^3x'\,\boldsymbol{v}'_t\boldsymbol{\cdot}\boldsymbol{B}'. \tag{3.43a–c}$$

Thus

$$\frac{\mathrm{d}H_{\mathrm{CNB}}}{\mathrm{d}t} = L^2U^2\bar{B}\frac{\mathrm{d}H'_{\mathrm{CNB}}}{\mathrm{d}t'} \quad \Rightarrow \quad \frac{\mathrm{d}H'_{\mathrm{CNB}}}{\mathrm{d}t'} = \frac{1}{L^2U^2\bar{B}}\frac{\mathrm{d}H_{\mathrm{CNB}}}{\mathrm{d}t}. \tag{3.44}$$

It follows that (3.30) can be written in the form

$$\begin{aligned} \frac{\mathrm{d}H'_{\mathrm{CNB}}}{\mathrm{d}t'} = \frac{1}{L^2U^2\bar{B}}\frac{\mathrm{d}H_{\mathrm{CNB}}}{\mathrm{d}t} = \int \Bigg\{ &\frac{1}{R_m}\left[\frac{\boldsymbol{v}'_t\boldsymbol{\cdot}\nabla'^2\boldsymbol{B}'}{4\pi} + \frac{J'^2}{\rho'T'}\boldsymbol{B}'\boldsymbol{\cdot}\boldsymbol{\nabla}'\sigma'\frac{E'_k}{E'_m}\frac{E_m}{E_k}\right] \\ &+ \frac{E'_k}{Q'_c}\frac{Q_c}{E_k}(\boldsymbol{B}'\boldsymbol{\cdot}\boldsymbol{\nabla}'\sigma')\frac{\nabla'^{2T'}}{\rho'T'} \\ &+ \frac{1}{R_e}\left[\frac{B'_i}{\rho'}\frac{\partial\sigma''_{ik}}{\partial x'_k} + (\boldsymbol{B}'\boldsymbol{\cdot}\boldsymbol{\nabla}'\sigma')\frac{\sigma''_{ik}}{\rho'T'}\frac{\partial v'_i}{\partial x'_k}\right]\Bigg\}\,\mathrm{d}^3x'. \end{aligned} \tag{3.45}$$

Thus, generally speaking, non-barotropic cross-helicity will change slowly for flows with both high Reynolds and high magnetic Reynolds numbers in which the heat conducted is small with respect to the kinetic energy of the flow. Indeed 'Increasing cross helicity with fixed fluctuation energy increases the time required for energy to cascade to smaller scales, reduces the cascade power, and increases the anisotropy of the small-scale fluctuations' (Chandran 2008). This has implications for the solar wind and solar corona (Chandran 2008).

It will also be of interest to study how another topological invariant, i.e. the magnetic helicity, changes for a flow of high Reynolds number. And how the rate of dissipation differs between those two quantities. Brief background regarding magnetic helicity is given below for the sake of the reader's convenience. The magnetic helicity is defined as

$$H_M \equiv \int \boldsymbol{A} \cdot \boldsymbol{B} \, \mathrm{d}^3 x, \tag{3.46}$$

where $\boldsymbol{A}$ is the magnetic vector potential, defined such that

$$\boldsymbol{B} = \nabla \times \boldsymbol{A}. \tag{3.47}$$

For an illustration of specific helical magnetic fields see Yahalom & Lynden-Bell (2008). After taking the temporal derivative of the magnetic helicity and simplifying the expressions, we obtain the well-known relation

$$\frac{\mathrm{d}H_M}{\mathrm{d}t} = -2\eta \int \boldsymbol{J} \cdot \boldsymbol{B} \, \mathrm{d}^3 x. \tag{3.48}$$

The above relation has been verified by many authors (Biskamp 1997; Akhmet'ev, Kunakovskaya & Kutvitskii 2009; Priest 2014; Verma 2019, 2021). It is clear from (3.48) that, generally speaking, the magnetic diffusivity leads to the non-conservation of magnetic helicity in non-ideal MHD. On the other hand, neither viscosity nor heat conductivity affect the conservation of magnetic helicity. We can easily recover the ideal MHD condition by putting magnetic diffusivity to zero, in which case it is evident that the magnetic helicity is conserved. Furthermore, the above result also shows that magnetic helicity is conserved even in non-ideal flows if the currents are orthogonal to the magnetic field i.e. $\boldsymbol{J} \cdot \boldsymbol{B} = 0$. In this case

$$\frac{\mathrm{d}H_M}{\mathrm{d}t} = 0. \tag{3.49}$$

If the magnetic field and magnetic current density are not strictly orthogonal then the magnetic helicity is only approximately conserved.

The above result can also be expressed in a dimensionless form in which we write the vector potential as

$$\boldsymbol{A} = \bar{A}\boldsymbol{A}', \quad \bar{A} = \bar{B}L. \tag{3.50a,b}$$

And thus

$$H_M = \bar{H}_M H'_M, \quad H'_M \equiv \int \boldsymbol{A}' \cdot \boldsymbol{B}' \, \mathrm{d}^3 x', \quad \bar{H}_M \equiv \bar{B}^2 L^4. \tag{3.51a–c}$$

For a similar dimensional analysis of magnetic helicity see Russell *et al.* (2015, (17)). It is straightforward to see that

$$\frac{\mathrm{d}H'_M}{\mathrm{d}t'} = -\frac{2}{R_m} \int \boldsymbol{J}' \cdot \boldsymbol{B}' \, \mathrm{d}^3 x'. \tag{3.52}$$

It follows that an approximate conservation of magnetic helicity is achievable at high magnetic Reynolds number and is independent ofthe values of the Reynolds number and total conducted heat. Thus the phenomenon of magnetic helicity conservation is much more general.

https://doi.org/10.1017/S002237782300123X Published online by Cambridge University Press

4. An application

We shall deal with the application in two stages with a helical stratified magnetic field; in the first we describe an ideal MHD flow following Yahalom & Qin (2021), then we assume a small magnetic diffusivity η (high magnetic Reynolds number) and discuss the implications for the flow. Finally, we calculate the magnetic and cross-helicities and discuss their relative rate of change.

4.1. *The ideal case*

We introduce a set of standard cylindrical coordinates R, ϕ, z, where $\hat{R}, \hat{\phi}, \hat{z}$ are the corresponding unit vectors. We further assume an MHD flow of uniform density ρ confined between the internal and external radii $a_{\rm in}$ and a, respectively, i.e. $a_{\rm in} < R < a$. Furthermore assume that the flow contains a helical stratified stationary magnetic field

$$\boldsymbol{B} = \begin{cases} 2B_{\perp}\left(1 - \dfrac{R}{a}\right)\hat{\phi} + B_{z0}\hat{z} & a_{\rm in} < R < a \\ 0 & \text{otherwise,} \end{cases} \tag{4.1}$$

in which $B_{z0}, B_{\perp}$ are constants. The magnetic field is contained in a cylinder of radius a and is independent of z. Furthermore, we assume that the planes $z = 0$ and $z = L$ can be identified such that a topological torus is created. In such a scenario, the only field lines that will be closed will satisfy the relation

$$\frac{n}{m} = \frac{B_{\perp}}{\pi R B_{z0}}\left(1 - \frac{R}{a}\right)L, \quad n, m \text{ integers}, \tag{4.2}$$

while lines not satisfying this relation will be surface filling.

In Yahalom & Qin (2021), we derive a stationary velocity field $\boldsymbol{v}$ that satisfies the stationary ideal versions of (2.4) and (2.2)

$$\nabla \times (\boldsymbol{v} \times \boldsymbol{B}) = 0, \tag{4.3}$$

$$\nabla \boldsymbol{\cdot} (\rho \boldsymbol{v}) = 0. \tag{4.4}$$

There, we arrived at the simple expression

$$\boldsymbol{v} = v_0 \frac{R}{a}\hat{\phi}, \tag{4.5}$$

where v_0 is a constant with dimensions of velocity. The ideal stationary version of (2.1) is given by

$$\rho(\boldsymbol{v} \boldsymbol{\cdot} \nabla)\boldsymbol{v} = -\nabla p + \frac{(\nabla \times \boldsymbol{B}) \times \boldsymbol{B}}{4\pi}. \tag{4.6}$$

This can be solved by the pressure function

$$p(R) = \frac{B_{\perp}^2}{\pi}\left(3\frac{R}{a} - \frac{R^2}{a^2} - \ln\left(\frac{R}{a}\right) - 2\right) + \frac{1}{2}\rho v_0^2\left(\frac{R^2}{a^2} - 1\right), \quad p(a) = 0. \tag{4.7}$$

Of course, $p(a_{\rm in}) \neq 0$, and thus one will need a rigid internal cylinder of radius $a_{\rm in}$ that can support such a pressure. We can now calculate the cross-helicity using (3.1), in which we

https://doi.org/10.1017/S002237782300123X Published online by Cambridge University Press

assume a uniform specific entropy such that $\boldsymbol{v}_t = \boldsymbol{v}$. Inserting (4.5) and (4.1) into (3.1) we arrive at the expression

$$H_{\mathrm{CNBI}} = \frac{\pi}{3} v_0 B_\perp \frac{L}{a^2} \left[a^4 - a_{\mathrm{in}}^3 (4a - 3a_{\mathrm{in}}) \right]. \tag{4.8}$$

In order to calculate the magnetic helicity, we need to calculate a vector potential, one possibility is given by

$$\boldsymbol{A} = \begin{cases} \dfrac{1}{2} B_{z0} R \hat{\phi} - 2B_\perp R \left(1 - \dfrac{R}{2a}\right) \hat{z} & a_{\mathrm{in}} < R < a \\ 0 & \text{otherwise}. \end{cases} \tag{4.9}$$

Inserting (4.1) and (4.9) into (3.46) we arrive at the result

$$H_{MI} = -\tfrac{2}{3} \pi L B_{z0} B_\perp (a - a_{\mathrm{in}}) \left[a^2 + a_{\mathrm{in}} a + a_{\mathrm{in}}^2 \right]. \tag{4.10}$$

Obviously, both magnetic helicity and magnetic cross-helicity do not change in time. The situation, however, is quite different when one considers non-ideal processes such as magnetic diffusion.

4.2. *The non-ideal case*

Let us assume a non-ideal magnetic diffusion; the magnetic field $\boldsymbol{B}_T$ will obviously be different from $\boldsymbol{B}$ and we may write it in the following form:

$$\boldsymbol{B}_T = \boldsymbol{B} + \eta \boldsymbol{B}_1. \tag{4.11}$$

In the above, $\boldsymbol{B}$ is given in (4.1) and is thus a stationary solution of an ideal MHD configuration. If we take the typical scale to be a and the typical velocity to be v_0, we can write the magnetic Reynolds number in the form

$$R_m = \frac{v_0 a}{\eta}, \quad \Rightarrow \quad \eta = \frac{v_0 a}{R_m}. \tag{4.12}$$

Thus, if we take the typical size of the magnetic fields $\boldsymbol{B}_T$ and $\boldsymbol{B}$ to be $\bar{B}_T = \bar{B} = B_{z0}$ and the typical size of $\boldsymbol{B}_1$ to be $\bar{B}_1 = B_{z0}/v_0 a$, we may write

$$\boldsymbol{B}'_T = \boldsymbol{B}' + \frac{1}{R_m} \boldsymbol{B}'_1. \tag{4.13}$$

We shall assume that the magnetic Reynolds number is large, such that the non-ideal correction is small. Now, $\boldsymbol{B}_T$ must satisfy (2.4)

$$\frac{\partial \boldsymbol{B}_T}{\partial t} = \nabla \times (\boldsymbol{v} \times \boldsymbol{B}_T) + \frac{\eta}{4\pi} \nabla^2 \boldsymbol{B}_T, \tag{4.14}$$

assuming that the velocity field is given by (4.5), and taking int account that $\boldsymbol{B}$ is stationary, we arrive at

$$\eta \frac{\partial \boldsymbol{B}_1}{\partial t} = \eta \nabla \times (\boldsymbol{v} \times \boldsymbol{B}_1) + \frac{\eta}{4\pi} \nabla^2 (\boldsymbol{B} + \eta \boldsymbol{B}_1). \tag{4.15}$$

Thus, η can be cancelled out and we obtain

$$\frac{\partial \boldsymbol{B}_1}{\partial t} = \nabla \times (\boldsymbol{v} \times \boldsymbol{B}_1) + \frac{1}{4\pi} \nabla^2 (\boldsymbol{B} + \eta \boldsymbol{B}_1). \tag{4.16}$$

Therefore, the term $\eta \boldsymbol{B}_1 = (B_{z0}/R_m) \boldsymbol{B}'_1$ can be neglected for high magnetic Reynolds

https://doi.org/10.1017/S002237782300123X Published online by Cambridge University Press

numbers. Thus, we arrive at the equation

$$\frac{\partial \boldsymbol{B}_1}{\partial t} = \nabla \times (\boldsymbol{v} \times \boldsymbol{B}_1) + \frac{1}{4\pi}\nabla^2 \boldsymbol{B}. \tag{4.17}$$

The source term of the above equation is, according to (4.1),

$$\frac{1}{4\pi}\nabla^2 \boldsymbol{B} = -\frac{B_\perp}{2\pi R^2}\hat{\phi}, \tag{4.18}$$

for every point $R < a$. Moreover, it is easy to show that, if at a specified time $t = 0$ we have $\boldsymbol{B}_1(\boldsymbol{x}, 0) = 0$, it follows that $B_{1R}(\boldsymbol{x}, t) = B_{1z}(\boldsymbol{x}, t) = 0$ for any time t. The equation for $B_{1\phi}$ is thus

$$\frac{\partial B_{1\phi}}{\partial t} = -\frac{B_\perp}{2\pi R^2}, \tag{4.19}$$

which can be trivially integrated

$$B_{1\phi} = -\frac{B_\perp}{2\pi R^2}t. \tag{4.20}$$

Thus the total magnetic field is

$$\boldsymbol{B}_T = \begin{cases} 2B_\perp\left(1 - \dfrac{R}{a} - \dfrac{\eta}{4\pi R^2}t\right)\hat{\phi} + B_{z0}\hat{z} & a_{\text{in}} < R < a \\ 0 & \text{otherwise.} \end{cases} \tag{4.21}$$

And thus the current density can be calculated using (2.7) to be

$$\boldsymbol{J}_T = \begin{cases} \dfrac{B_\perp}{2\pi R}\left(1 - \dfrac{2R}{a} + \dfrac{\eta}{4\pi R^2}t\right)\hat{z} & a_{\text{in}} < R < a \\ 0 & \text{otherwise.} \end{cases} \tag{4.22}$$

Thus one can calculate the time-dependent pressure using (2.1)

$$\begin{aligned} p(R, t) = {} & \frac{B_\perp^2}{\pi}\left(3\frac{R}{a} - \frac{R^2}{a^2} - \ln\left(\frac{R}{a}\right) - 2 + \frac{\eta t}{4\pi a}\left(\frac{1}{R} - \frac{1}{a}\right) - \frac{\eta^2 t^2}{96\pi^2}\left(\frac{1}{R^6} - \frac{1}{a^6}\right)\right) \\ & + \frac{1}{2}\rho v_0^2\left(\frac{R^2}{a^2} - 1\right), \quad p(a, t) = 0. \end{aligned} \tag{4.23}$$

Thus the internal cylinder must sustain the above time-dependent pressure.

Now, to calculate the magnetic helicity we need a vector potential; this can be similarly obtained as in the ideal case in the form

$$\boldsymbol{A}_T = \begin{cases} \dfrac{1}{2}B_{z0}R\hat{\phi} - 2B_\perp R\left(1 - \dfrac{R}{2a} + \dfrac{\eta t}{4\pi R^2}\right)\hat{z} & a_{\text{in}} < R < a \\ 0 & \text{otherwise.} \end{cases} \tag{4.24}$$

Inserting (4.21) and (4.24) into (3.46) will result in a time-dependent magnetic helicity

$$H_{\text{MT}} = -\frac{2}{3}\pi L B_{z0} B_\perp (a - a_{\text{in}})\left[a^2 + a_{\text{in}}a + a_{\text{in}}^2 + \frac{9\eta t}{4\pi}\right]. \tag{4.25}$$

https://doi.org/10.1017/S002237782300123X Published online by Cambridge University Press

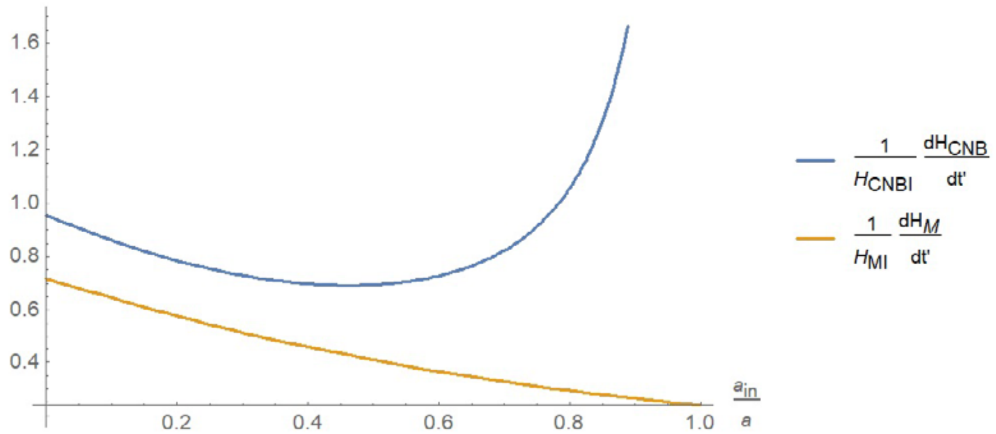

FIGURE 1. Comparison of $|(1/H_{\mathrm{MI}})(\mathrm{d}H_{\mathrm{MT}}/\mathrm{d}t')|$ with $|(1/H_{\mathrm{CNBI}})(\mathrm{d}H_{\mathrm{CNBT}}/\mathrm{d}t')|$ for $R_m = 1$.

The time derivative of the above magnetic helicity is

$$\frac{\mathrm{d}H_{MT}}{\mathrm{d}t} = -\frac{3}{2} L B_{z0} B_{\perp} (a - a_{\mathrm{in}}) \eta. \tag{4.26}$$

Similarly, inserting (4.21) and (4.5) into (3.1) will result in a time-dependent cross-helicity

$$H_{\mathrm{CNBT}} = 4\pi v_0 B_{\perp} \frac{L}{a} \left[\frac{1}{3}(a^3 - a_{\mathrm{in}}^3) - \frac{1}{4a}(a^4 - a_{\mathrm{in}}^4) - \frac{\eta t}{4\pi}(a - a_{\mathrm{in}}) \right], \tag{4.27}$$

with a time derivative of

$$\frac{\mathrm{d}H_{\mathrm{CNBT}}}{\mathrm{d}t} = -v_0 B_{\perp} \frac{L}{a} (a - a_{\mathrm{in}}) \eta. \tag{4.28}$$

It is interesting to compare which of the topological quantities is better preserved given some high Reynolds number (and neglecting viscosity and heat conduction). To this end we compare

$$\left| \frac{1}{H_{\mathrm{MI}}} \frac{\mathrm{d}H_{MT}}{\mathrm{d}t'} \right| = \frac{9}{4\pi R_m (1 + a'_{\mathrm{in}} + a'^2_{\mathrm{in}})}, \quad a'_{\mathrm{in}} \equiv \frac{a_{\mathrm{in}}}{a}, \quad t' = t\frac{v_0}{a}, \tag{4.29a–c}$$

with

$$\left| \frac{1}{H_{\mathrm{CNBI}}} \frac{\mathrm{d}H_{\mathrm{CNBT}}}{\mathrm{d}t'} \right| = \frac{3(1 - a'_{\mathrm{in}})}{\pi R_m \left[1 - a'^3_{\mathrm{in}}(4 - 3a'_{\mathrm{in}}) \right]}. \tag{4.30}$$

Both the above quantities are inversely proportional to the magnetic Reynolds number R_m. The results for $Rm = 1$ are depicted in figure 1, which illustrates that the relative rates of change of both quantities are about the same, with a slight advantage to the magnetic helicity depending on the particular geometry of the configuration. It is shown that, for the right pressure profile, both magnetic helicity and cross-helicity are of comparable importance. The higher the magnetic Reynolds number, the more ideal the flow is.

5. Topological bounds

Topological quantities serve as lower bounds on MHD 'energies' thus preventing some types of instabilities developing. For example, Moffatt (1992) shows that the 'energy' is bounded from below by the magnetic helicity using the Cauchy–Schwarz inequality

$$H_M = \int \boldsymbol{B} \boldsymbol{\cdot} \boldsymbol{A} \, \mathrm{d}^3 x \leqslant \sqrt{\int \boldsymbol{A}^2 \, \mathrm{d}^3 x} \sqrt{\int \boldsymbol{B}^2 \, \mathrm{d}^3 x}. \tag{5.1}$$

In addition, it was shown by Yahalom (2017*a*) that

$$H_M = \int \boldsymbol{B} \boldsymbol{\cdot} \boldsymbol{A} \, \mathrm{d}^3 x \leqslant \frac{1}{2} \int \left(\boldsymbol{B}^2 + \boldsymbol{A}^2\right) \mathrm{d}^3 x. \tag{5.2}$$

A similar analysis can be done for the non-barotropic cross-helicity. It is easy to show that the 'energy' is bounded from below by the cross-helicity as follows:

$$H_{\mathrm{CNB}} = \int \boldsymbol{B} \boldsymbol{\cdot} \boldsymbol{v}_t \, \mathrm{d}^3 x \leqslant \frac{1}{2} \int \left(\boldsymbol{B}^2 + \boldsymbol{v}_t{}^2\right) \mathrm{d}^3 x, \tag{5.3}$$

$$H_{\mathrm{CNB}} = \int \boldsymbol{B} \boldsymbol{\cdot} \boldsymbol{v}_t \, \mathrm{d}^3 x \leqslant \sqrt{\int \boldsymbol{v}_t{}^2 \, \mathrm{d}^3 x} \sqrt{\int \boldsymbol{B}^2 \, \mathrm{d}^3 x}. \tag{5.4}$$

In this sense, a configuration with a highly complicated topology is more stable since its energy is bounded from below. The current paper discusses the constancy of the topological invariants when MHD flow is not ideal, with obvious implications for the applicability of the above constraints.

6. The Z pinch and cross-helicity

Some types of plasma devices are dependent on fast changes ('instabilities') to generate physical effects. One of those is the Z pinch, in which a current flowing in the axial direction (z direction) through a plasma is used to generate an azimuthal magnetic field which produces a Lorentz force compressing the plasma column. This was suggested initially as a fusion configuration, and lately as a neutronsource (Zhang *et al.* 2019).

We consider a cylindrical coordinate system as in § 4, however, now we assume

$$\boldsymbol{B} = B_\phi(R)\hat{\phi}, \tag{6.1}$$

which is an azimuthal magnetic field which depends only on the radial coordinate R. This is associated with a current according to (2.7)

$$\boldsymbol{J} = J_z \hat{z}, \quad J_z(R) = \frac{1}{4\pi R} \frac{\partial (R B_\phi)}{\partial R}. \tag{6.2a,b}$$

We thus obtain a Lorentz force density in the radial direction

$$\boldsymbol{f}_L = \boldsymbol{J} \times \boldsymbol{B} = f_{\mathrm{LR}} \hat{R}, \quad f_{\mathrm{LR}}(R) = -\frac{1}{4\pi} \left[\frac{\partial}{\partial R} \left(\frac{1}{2} B_\phi^2 \right) + \frac{B_\phi^2}{R} \right]. \tag{6.3a,b}$$

Hence, by carefully crafting the radial distribution of J_z, we obtain an inward radial force, which will cause an inward radial acceleration, and hence aradial velocity and

https://doi.org/10.1017/S002237782300123X Published online by Cambridge University Press

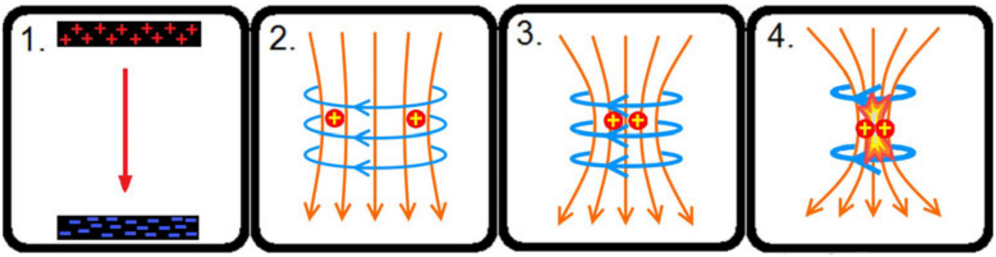

FIGURE 2. Pinch effect in four steps. 1. Current generation by electrodes. 2. The current (presented by orange line) generated by a magnetic field (presented by blue lines). 3. The Lorentz force compresses the plasma. 4. If high enough density and temperature are achieved for a sufficient time, fusion occurs.

displacement leading to implosion. The implosion will lead hopefully to a high density and temperature and thus to fusion and neutron production (see figure 2).

Since the velocity vector is expected to be in the radial direction, in an ideal case, no cross-helicityis expected to develop and thus the configuration seems topologically trivial. However, in practice, some azimuthal velocity may exist with the associated cross-helicity. It is the effect of this cross-helicity which we now investigate. Let us suppose a velocity field of the form

$$\boldsymbol{v} = v_R(R,t)\hat{R} + v_\phi(R),\hat{\phi} \tag{6.4}$$

in which we take for simplicity the azimuthal velocity component to be stationary. We shall assume that no potential force or viscous force issignificant, and that the pressure $p(R)$ depends only on the radial coordinate. In this case, there is no force component in the azimuthal direction and we obtain

$$\left(\frac{\mathrm{d}\boldsymbol{v}}{\mathrm{d}t}\right)_\phi = ((\boldsymbol{v}\cdot\nabla)\boldsymbol{v})_\phi = v_R\frac{\partial v_\phi}{\partial R} + \frac{1}{R}v_R v_\phi = 0. \tag{6.5}$$

This is easily solved for the case $v_R \neq 0$ in terms of the azimuthal velocity at a single point R_m

$$v_\phi(R) = v_\phi(R_m)\left(\frac{R_m}{R}\right). \tag{6.6}$$

Assuming a barotropic equation of state, the cross-helicity given in (3.1) can be calculated as follows:

$$\begin{aligned} H_{\mathrm{CNB}} &= \int \mathrm{d}^3x\, \boldsymbol{v}_t\cdot\boldsymbol{B} = \int \mathrm{d}^3x\, v_\phi B_\phi = \int \mathrm{d}z'\, R'\,\mathrm{d}R'\,\mathrm{d}\phi'\, v_\phi B_\phi \\ &= 2\pi R_m v_\phi(R_m) L \int B_\phi(R')\,\mathrm{d}R'. \end{aligned} \tag{6.7}$$

In the above, L is the length of the plasma column. Taking R_m to be a radial distance beyond which the azimuthal magnetic field vanishes and defining an average azimuthal

https://doi.org/10.1017/S002237782300123X Published online by Cambridge University Press

magnetic field as

$$\langle B_\phi \rangle = \frac{1}{R_m} \int_0^{R_m} B_\phi(R')\,\mathrm{d}R', \tag{6.8}$$

we have

$$v_\phi(R) = \frac{H_{\mathrm{CNB}}}{2\pi R_m L \langle B_\phi \rangle R}. \tag{6.9}$$

Next, we shall write the equation for the radial velocity component, which is derived from (2.1)

$$\left(\frac{\mathrm{d}\boldsymbol{v}}{\mathrm{d}t}\right)_R = \frac{\partial v_R}{\partial t} + ((\boldsymbol{v} \cdot \nabla)\boldsymbol{v})_R = -\frac{1}{\rho}\frac{\partial p(R)}{\partial R} - \frac{J_z B_\phi}{\rho}. \tag{6.10}$$

Notice that

$$((\boldsymbol{v} \cdot \nabla)\boldsymbol{v})_R = \frac{1}{2}\frac{\partial v_R^2}{\partial R} - \frac{v_\phi^2}{R}. \tag{6.11}$$

It follows that

$$\frac{\partial v_R}{\partial t} = -\frac{1}{2}\frac{\partial v_R^2}{\partial R} + \frac{v_\phi^2}{R} - \frac{1}{\rho}\frac{\partial p(R)}{\partial R} - \frac{J_z B_\phi}{\rho}. \tag{6.12}$$

Or, more explicitly,

$$\frac{\partial v_R}{\partial t} = -\frac{1}{2}\frac{\partial v_R^2}{\partial R} + \frac{H_{\mathrm{CNB}}^2}{(2\pi R_m L \langle B_\phi \rangle)^2 R^3} - \frac{1}{\rho}\frac{\partial p(R)}{\partial R} - \frac{1}{4\pi\rho}\left(\frac{1}{2}\frac{\partial B_\phi^2}{\partial R} + \frac{B_\phi^2}{R}\right). \tag{6.13}$$

From a dynamical point of view, the cross-helicity has a negative effect because, for a fast pinch, we would like to have a negatively large $\partial v_R/\partial t < 0$; however, the cross-helicity will diminish the negativity of the right-hand side and thus has an adverse effect. As the density in the pinch core increases, the pressure gradient will build up, eventually stopping the implosion and thus the radial velocity will vanish $v_r = 0$. In that case

$$\left|\frac{1}{\rho}\frac{\partial p(R)}{\partial R}\right| = -\frac{1}{\rho}\frac{\partial p(R)}{\partial R} = -\frac{H_{\mathrm{CNB}}^2}{(2\pi R_m L \langle B_\phi \rangle)^2 R^3} + \frac{1}{4\pi\rho}\left(\frac{1}{2}\frac{\partial B_\phi^2}{\partial R} + \frac{B_\phi^2}{R}\right). \tag{6.14}$$

https://doi.org/10.1017/S002237782300123X Published online by Cambridge University Press

So the maximal pressure gradient (and therefore the maximal core density) diminishes due to the cross-helicity. We underline that, in the Z pinch scenario, the dissipation of the cross-helicity as described in (3.30) has a positive effect, allowing us to achieve a higher core density faster.

7. Summary and concluding remarks

The conservation of topological constants of motion such as the non-barotropic cross-helicity and magnetic helicity imposes constraints on the MHD flow and thus affects its stability (Yahalom 2017*b*). In his important review paper 'Physics of magnetically confined plasmas', A. H. Boozer (Boozer 2005) states that: 'A spiky current profile causes a rapid dissipation of energy relative to magnetic helicity. If the evolution of a magnetic field is rapid, then it must be at constant helicity'.

To achieve fusion, one needs to achieve a stable plasma which has the needed temperature and density to sustain fusion. Usually, this is difficult to achieve for a long enough duration at Earth conditions in Earth's laboratory. A flow with a non-trivial topology seems to be more stable as the energy of the flow is bounded from below. Usually, topological conservation laws are used in order to deduce lower bounds on the 'energy' of the flow. Those bounds are only approximate in non-ideal flows but, due to their topological nature, simulations show that they are approximately conserved even when the 'energy' is not.

To summarize, we have analytically examined the evolution of generalized cross-helicity for non-ideal compressible MHD by taking resistive heating, heat conduction and viscous effects into account. To achieve the aforementioned aim, first, we have derived a specific entropy equation which is valid in non-ideal MHD flow with the help of an energy equation. After that, using the basic MHD equations and the definition of non-barotropic cross-helicity, we have derived the rate of change of generalized cross-helicity with time. We have shown that the helicities are not conserved in non-ideal MHD flow and their time derivatives depend only on non-ideal processes. One can easily recover ideal MHD conditions by putting all of the non-ideal constants to zero.

Magnetic and non-barotropic cross-helicities differ; the magnetic helicity is only affected by magnetic diffusivity while the non-barotropic cross-helicity is dependent on viscosity and heat conduction as well (except for special cases), making it more susceptible to change over time. A dimensional analysis shows that, for a magnetic helicity 'slow change', one needs only a high magnetic Reynolds number, but this will not suffice for a 'slow change' of non-barotropic cross-helicity. The latter case requires in addition a high Reynolds number (non-magnetic) as well as limitations to the amount of heat conducted with respect to the flow kinetic energy.

The generalized cross-helicity conservation law may find potential uses in solar MHD. Under the influence of rotation and baroclinic instability, events such as magnetic tornadoes can occur. Within these tornadoes, vorticity is generated as a result of the baroclinic term (Webb & Mace 2015). The relevance of non-zero cross-helicity in astrophysical and space plasma phenomena is nicely explained by Yokoi (2013) and references therein. It is believed that non-barotropic cross-helicity, which unlike standard cross-helicity can only be modified by non-ideal processes that are usually slower, can be even more useful. For recent developments, one can refer to Heinonen *et al.* (2021). Perez & Boldyrev (2009) has discussed its role in MHD turbulence by high resolution direct numerical simulations. However, space plasma is generally not ideal in nature and the real picture can be understood only by studying the helicity evolution in a non-ideal environment. Many studies in the literature have shown that cross-helicity is correlated to the self-production of turbulence. Biskamp (2003) has presented a decay law for MHD turbulence with the help of the conservation law for magnetic helicity. Variation in energy flux is also adopted by Verma (2004) to study the decay law in MHD turbulence. Mizeva, Stepanov & Frik (2009) has discussed the effect of cross-helicity on the cascade process in MHD turbulence. They showed from numerical results that ‘cross helicity blocks the spectral energy transfer in MHD turbulence and results in energy accumulation in the system. This accumulation proceeds until the vortex intensification compensates the decreasing efficiency of nonlinear interactions’. The impact of non-zero cross-helicity on MHD turbulence is unparalleled and affects the global dynamics. Briard & Gomez (2018) examined the effect of cross-helicity on the decay of isotropic MHD turbulence and concluded that an initial non-zero cross-helicity makes for imbalanced MHD turbulence. The subtle anisotropic effect of cross-helicity could be the cause of this. In this paper, we have given simple examples making non-zero cross helicity easy to analyse but it is not too simple in the sense that it has both non-trivial magnetic helicity and non-trivial cross-helicity. We give an exact analytic solution of ideal MHD, which is not a trivial since the equations of MHD (even ideal) are nonlinear partial differential equations. We also give an approximate solution (for high magnetic Reynolds number) for non-ideal flows. Then, we show that both quantities change by about the same fractions (that is, in percentage with respect to their initial values). This corresponds well with our general result that magnetic and cross-helicities both change inverse proportionally with the magnetic Reynolds number, provided viscosity and heat conductivity can be neglected. The question as to whether this is a reasonable assumption in specific astrophysical or Earth-based MHD flow is beyond the scope of the current paper. In addition, we mentioned the ideal inequality constraint that is imposed by magnetic helicity and non-barotropic cross-helicity on MHD flows. Finally, we discussed the adverse effect of cross-helicity on the Z pinch.

For better insight into possible applications of the non-barotropic cross-helicity, the authors plan to develop variational principles for non-ideal MHD in the future. Our aim is to use them for the analysis of the stability of non-ideal MHD configurations. As for designing efficient numerical schemes for integrating the equations of fluid dynamics and MHD, one may follow the approach described in Yahalom (2003). Analysing the dynamics of the new generalized non-barotropic χ and η cross-helicities recently developed by Yahalom & Qin (2021) in the non-ideal case will also be a part of future work, as well as attention to their local/global forms. To this end, we recall that both magnetic helicity has local form, that is, the magnetic helicity per unit of magnetic flux $[\zeta]$ and non-barotropic crosshelicity per unit of magnetic flux $[\nu]$, which are both conserved quantities in ideal flows (Yahalom 2017*b*, (27) and (36)).

Acknowledgements

Editor Steve Tobias thanks the referees for their advice in evaluating this article.

Declaration of interests

The authors report no conflict of interest.

Appendix A. Variational approach to ideal non-barotropic magnetohydrodynamics

In the following, we repeat for the reader’s convenience the variational analysis that can be found in Yahalom (2016*b*,*a*) and which generalizes the approach of Yahalom &

Lynden-Bell (2008) for the non-barotropic case. Consider the action

$$\left.\begin{aligned} A &\equiv \int \mathcal{L}\, \mathrm{d}^3x\, \mathrm{d}t, \\ \mathcal{L} &\equiv \mathcal{L}_1 + \mathcal{L}_2, \\ \mathcal{L}_1 &\equiv \rho\left(\frac{1}{2}\boldsymbol{v}^2 - \varepsilon(\rho, s)\right) + \frac{\boldsymbol{B}^2}{8\pi}, \\ \mathcal{L}_2 &\equiv \nu\left[\frac{\partial\rho}{\partial t} + \boldsymbol{\nabla}\boldsymbol{\cdot}(\rho\boldsymbol{v})\right] - \rho\alpha\frac{\mathrm{d}\chi}{\mathrm{d}t} - \rho\beta\frac{\mathrm{d}\eta_0}{\mathrm{d}t} - \rho\sigma\frac{\mathrm{d}s}{\mathrm{d}t} - \frac{\boldsymbol{B}}{4\pi}\boldsymbol{\cdot}\boldsymbol{\nabla}\chi\times\boldsymbol{\nabla}\eta_0. \end{aligned}\right\} \tag{A1}$$

In the above, ε is the specific internal energy (internal energy per unit of mass). The reader is reminded of the following thermodynamic relations which will become useful later:

$$\left.\begin{aligned} \mathrm{d}\varepsilon &= T\,\mathrm{d}s - P\,\mathrm{d}\frac{1}{\rho} = T\,\mathrm{d}s + \frac{P}{\rho^2}\mathrm{d}\rho \\ \frac{\partial\varepsilon}{\partial s} &= T, \quad \frac{\partial\varepsilon}{\partial\rho} = \frac{P}{\rho^2} \\ w &= \varepsilon + \frac{P}{\rho} = \varepsilon + \frac{\partial\varepsilon}{\partial\rho}\rho = \frac{\partial(\rho\varepsilon)}{\partial\rho} \\ \mathrm{d}w &= \mathrm{d}\varepsilon + \mathrm{d}\left(\frac{P}{\rho}\right) = T\,\mathrm{d}s + \frac{1}{\rho}\mathrm{d}P. \end{aligned}\right\} \tag{A2}$$

Obviously, $\nu, \alpha, \beta, \sigma$ are Lagrange multipliers which were inserted in such a way that the variational principle will yield the following equations:

$$\left.\begin{aligned} \frac{\partial\rho}{\partial t} + \boldsymbol{\nabla}\boldsymbol{\cdot}(\rho\boldsymbol{v}) &= 0, \\ \rho\frac{\mathrm{d}\chi}{\mathrm{d}t} &= 0, \\ \rho\frac{\mathrm{d}\eta_0}{\mathrm{d}t} &= 0, \\ \rho\frac{\mathrm{d}s}{\mathrm{d}t} &= 0. \end{aligned}\right\}. \tag{A3}$$

It is not assumed that $\nu, \alpha, \beta, \sigma$ are single valued. Provided ρ is not null, those are just the continuity equation (2.2), entropy conservation and the conditions that Sakurai's functions are comoving. Taking the variational derivative with respect to $\boldsymbol{B}$, we see that

$$\boldsymbol{B} = \hat{\boldsymbol{B}} \equiv \boldsymbol{\nabla}\chi\times\boldsymbol{\nabla}\eta_0. \tag{A4}$$

Hence, $\boldsymbol{B}$ is in Sakurai's form and satisfies (2.3). It can be easily shown that, provided that $\boldsymbol{B}$ is in the form given in (A4), and (A3) are satisfied, then also (2.4) is satisfied for zero magnetic diffusivity $\eta = 0$.

For the time being we have shown that all of the equations of non-barotropic magnetohydrodynamics can be obtained from the above variational principle, except Euler's equations. We will now show that Euler's equations can be derived from the above

https://doi.org/10.1017/S002237782300123X Published online by Cambridge University Press

variational principle as well. Let us take an arbitrary variational derivative of the above action with respect to $\boldsymbol{v}$, this will result in

$$\delta_{\boldsymbol{v}} A=\int \mathrm{d}t\left\{\int \mathrm{d}^3x\,\mathrm{d}t\,\rho\,\delta\boldsymbol{v}\cdot[\boldsymbol{v}-\boldsymbol{\nabla}\nu-\alpha\boldsymbol{\nabla}\chi-\beta\boldsymbol{\nabla}\eta_0-\sigma\boldsymbol{\nabla}s]+\oint \mathrm{d}\boldsymbol{S}\cdot\delta\boldsymbol{v}\rho\nu \right.$$
$$\left.+\int \mathrm{d}\boldsymbol{\Sigma}\cdot\delta\boldsymbol{v}\rho[\nu]\right\}. \tag{A5}$$

The integral $\oint \mathrm{d}\boldsymbol{S}\cdot\delta\boldsymbol{v}\rho\nu$ vanishes in many physical scenarios. In the case of astrophysical flows, this integral will vanish since $\rho=0$ on the flow boundary, in the case of a fluid contained in a vessel with no-flux boundary conditions, $\delta\boldsymbol{v}\cdot\hat{n}=0$ is induced ($\hat{n}$ is a unit vector normal to the boundary). The surface integral $\int \mathrm{d}\boldsymbol{\Sigma}$ on the cut of ν vanishes in the case that ν is single valued and $[\nu]=0$ as is the case for some flow topologies. In the case that ν is not single valued, only a Kutta type velocity perturbation (Yahalom, Pinhasi & Kopylenko 2005) in which the velocity perturbation is parallel to the cut will cause the cut integral to vanish. An arbitrary velocity perturbation on the cut will indicate that $\rho=0$ on this surface,which is contradictory to the fact that a cut surface is to some degree arbitrary, as is the case for the zero line of an azimuthal angle. We will show later that the 'cut' surface is co-moving with the flow, hence it may become quite complicated. This uneasy situation may be somewhat be less restrictive when the flow has some symmetry properties.

Provided that the surface integrals do vanish and that $\delta_{\boldsymbol{v}}A=0$ for an arbitrary velocity perturbatio, we see that $\boldsymbol{v}$ must have the following form:

$$\boldsymbol{v}=\hat{\boldsymbol{v}}\equiv\boldsymbol{\nabla}\nu+\alpha\boldsymbol{\nabla}\chi+\beta\boldsymbol{\nabla}\eta_0+\sigma\boldsymbol{\nabla}s. \tag{A6}$$

The above equation is reminiscent of Clebsch representation in non-magnetic fluids (Clebsch 1857, 1859). Let us now take the variational derivative with respect to the density ρ, we obtain

$$\delta_\rho A=\int \mathrm{d}^3x\,\mathrm{d}t\,\delta\rho\left[\frac{1}{2}\boldsymbol{v}^2-w-\frac{\partial\nu}{\partial t}-\boldsymbol{v}\cdot\boldsymbol{\nabla}\nu\right]$$
$$+\int \mathrm{d}t\oint \mathrm{d}\boldsymbol{S}\cdot\boldsymbol{v}\delta\rho\nu+\int \mathrm{d}t\int \mathrm{d}\boldsymbol{\Sigma}\cdot\boldsymbol{v}\delta\rho[\nu]+\int \mathrm{d}^3x\,\nu\delta\rho|_{t_0}^{t_1}. \tag{A7}$$

Hence, provided that $\oint \mathrm{d}\boldsymbol{S}\cdot\boldsymbol{v}\delta\rho\nu$ vanishes on the boundary of the domain and $\int \mathrm{d}\boldsymbol{\Sigma}\cdot\boldsymbol{v}\delta\rho[\nu]$ vanishes on the cut of ν, in the case that ν is not single valued[1] , at the initial and final times the following equation must be satisfied:

$$\frac{\mathrm{d}\nu}{\mathrm{d}t}=\frac{1}{2}\boldsymbol{v}^2-w. \tag{A8}$$

Since the right-hand side of the above equation is single valued as it is made of physical quantities, we conclude that

$$\frac{\mathrm{d}[\nu]}{\mathrm{d}t}=0. \tag{A9}$$

Hence, the cut value is co-moving with the flow and thus the cut surface may become arbitrarily complicated. This uneasy situation may be somewhat be less restrictive when the flow has some symmetry properties.

[1]Which entails either a Kutta type condition for the velocity in contradiction to the 'cut' being an arbitrary surface, or a vanishing density perturbation on the cut.

https://doi.org/10.1017/S002237782300123X Published online by Cambridge University Press

Finally, we have to calculate the variation with respect to both χ and η_0, this will lead us to the following results:

$$\begin{aligned}
\delta_\chi A &= \int \mathrm{d}^3x\, \mathrm{d}t \delta\chi \left[\frac{\partial(\rho\alpha)}{\partial t} + \boldsymbol{\nabla}\boldsymbol{\cdot}(\rho\alpha\boldsymbol{v}) - \boldsymbol{\nabla}\eta_0 \boldsymbol{\cdot} \boldsymbol{J}\right] \\
&\quad + \int \mathrm{d}t \oint \mathrm{d}\boldsymbol{S}\boldsymbol{\cdot}\left[\frac{\boldsymbol{B}}{4\pi}\times\boldsymbol{\nabla}\eta_0 - \boldsymbol{v}\rho\alpha\right]\delta\chi \\
&\quad + \int \mathrm{d}t \int \mathrm{d}\boldsymbol{\Sigma}\boldsymbol{\cdot}\left[\frac{\boldsymbol{B}}{4\pi}\times\boldsymbol{\nabla}\eta_0 - \boldsymbol{v}\rho\alpha\right][\delta\chi] - \int \mathrm{d}^3x\, \rho\alpha\delta\chi|_{t_0}^{t_1},
\end{aligned} \tag{A10}$$

$$\begin{aligned}
\delta_{\eta_0} A &= \int \mathrm{d}^3x\, \mathrm{d}t \delta\eta_0 \left[\frac{\partial(\rho\beta)}{\partial t} + \boldsymbol{\nabla}\boldsymbol{\cdot}(\rho\beta\boldsymbol{v}) + \boldsymbol{\nabla}\chi \boldsymbol{\cdot} \boldsymbol{J}\right] \\
&\quad + \int \mathrm{d}t \oint \mathrm{d}\boldsymbol{S}\boldsymbol{\cdot}\left[\boldsymbol{\nabla}\chi\times\frac{\boldsymbol{B}}{4\pi} - \boldsymbol{v}\rho\beta\right]\delta\eta_0 \\
&\quad + \int \mathrm{d}t \int \mathrm{d}\boldsymbol{\Sigma}\boldsymbol{\cdot}\left[\boldsymbol{\nabla}\chi\times\frac{\boldsymbol{B}}{4\pi} - \boldsymbol{v}\rho\beta\right][\delta\eta_0] - \int \mathrm{d}^3x\, \rho\beta\delta\eta_0|_{t_0}^{t_1}.
\end{aligned} \tag{A11}$$

Provided that the correct temporal and boundary conditions are met with respect to the variations $\delta\chi$ and $\delta\eta_0$ on the domain boundary and on the cuts, in the case that some (or all) of the relevant functions are non-single valued, we obtain the following set of equations:

$$\frac{\mathrm{d}\alpha}{\mathrm{d}t} = \frac{\boldsymbol{\nabla}\eta_0\boldsymbol{\cdot}\boldsymbol{J}}{\rho}, \quad \frac{\mathrm{d}\beta}{\mathrm{d}t} = -\frac{\boldsymbol{\nabla}\chi\boldsymbol{\cdot}\boldsymbol{J}}{\rho}, \tag{A12a,b}$$

in which the continuity equation (2.2) was taken into account. By correct temporal conditions we mean that both $\delta\eta_0$ and $\delta\chi$ vanish at the initial and final times. As for the boundary conditions which are sufficient to make the boundary term vanish, one can consider the case that the boundary is at infinity and both $\boldsymbol{B}$ and ρ vanish. Another possibility is that the boundary is impermeable and perfectly conducting. A sufficient condition for the integral over the 'cuts' to vanish is to use variations $\delta\eta_0$ and $\delta\chi$, which are single valued. It can be shown that χ can always be taken to be single valued, hence taking $\delta\chi$ to be single valued is no restriction at all. In some topologies η_0 is not single valued and in those cases a single valued restriction on $\delta\eta_0$ is sufficient to make the cut term null.

Finally, we take a variational derivative with respect to the entropy s

$$\begin{aligned}
\delta_s A &= \int \mathrm{d}^3x\, \mathrm{d}t\delta s \left[\frac{\partial(\rho\sigma)}{\partial t} + \boldsymbol{\nabla}\boldsymbol{\cdot}(\rho\sigma\boldsymbol{v}) - \rho T\right] + \int \mathrm{d}t \oint \mathrm{d}\boldsymbol{S}\boldsymbol{\cdot}\rho\sigma\boldsymbol{v}\delta s \\
&\quad - \int \mathrm{d}^3x\, \rho\sigma\delta s|_{t_0}^{t_1}.
\end{aligned} \tag{A13}$$

We notice that, according to (A6), σ is single valued and hence no cuts are needed. Taking into account the continuity equation (2.2) we obtain for locations in which the density ρ is not null the result

$$\frac{\mathrm{d}\sigma}{\mathrm{d}t} = T, \tag{A14}$$

provided that $\delta_s A$ vanishes for an arbitrary δs, this is the same as (3.2).

https://doi.org/10.1017/S002237782300123X Published online by Cambridge University Press

Appendix B. Euler's equations

We shall now show that a velocity field given by (A6), such that the equations for $\alpha, \beta, \chi, \eta_0, \nu, \sigma, s$ satisfy the corresponding equations (A3), (A8), (A12*a*,*b*), (A14) must satisfy Euler's equations. Let us calculate the material derivative of $\boldsymbol{v}$

$$\frac{\mathrm{d}\boldsymbol{v}}{\mathrm{d}t} = \frac{\mathrm{d}\boldsymbol{\nabla}\nu}{\mathrm{d}t} + \frac{\mathrm{d}\alpha}{\mathrm{d}t}\boldsymbol{\nabla}\chi + \alpha\frac{\mathrm{d}\boldsymbol{\nabla}\chi}{\mathrm{d}t} + \frac{\mathrm{d}\beta}{\mathrm{d}t}\boldsymbol{\nabla}\eta_0 + \beta\frac{\mathrm{d}\boldsymbol{\nabla}\eta_0}{\mathrm{d}t} + \frac{\mathrm{d}\sigma}{\mathrm{d}t}\boldsymbol{\nabla}s + \sigma\frac{\mathrm{d}\boldsymbol{\nabla}s}{\mathrm{d}t}. \tag{B1}$$

It can be easily shown that

$$\left.\begin{aligned}
\frac{\mathrm{d}\boldsymbol{\nabla}\nu}{\mathrm{d}t} &= \boldsymbol{\nabla}\frac{\mathrm{d}\nu}{\mathrm{d}t} - \boldsymbol{\nabla}v_k\frac{\partial\nu}{\partial x_k} = \boldsymbol{\nabla}\left(\frac{1}{2}\boldsymbol{v}^2 - w\right) - \boldsymbol{\nabla}v_k\frac{\partial\nu}{\partial x_k},\\
\frac{\mathrm{d}\boldsymbol{\nabla}\eta_0}{\mathrm{d}t} &= \boldsymbol{\nabla}\frac{\mathrm{d}\eta_0}{\mathrm{d}t} - \boldsymbol{\nabla}v_k\frac{\partial\eta_0}{\partial x_k} = -\boldsymbol{\nabla}v_k\frac{\partial\eta_0}{\partial x_k},\\
\frac{\mathrm{d}\boldsymbol{\nabla}\chi}{\mathrm{d}t} &= \boldsymbol{\nabla}\frac{\mathrm{d}\chi}{\mathrm{d}t} - \boldsymbol{\nabla}v_k\frac{\partial\chi}{\partial x_k} = -\boldsymbol{\nabla}v_k\frac{\partial\chi}{\partial x_k},\\
\frac{\mathrm{d}\boldsymbol{\nabla}s}{\mathrm{d}t} &= \boldsymbol{\nabla}\frac{\mathrm{d}s}{\mathrm{d}t} - \boldsymbol{\nabla}v_k\frac{\partial s}{\partial x_k} = -\boldsymbol{\nabla}v_k\frac{\partial s}{\partial x_k},
\end{aligned}\right\} \tag{B2}$$

in which x_k is a Cartesian coordinate and a summation convention is assumed. Inserting the result from (B2) and (A3) into (B1) yields

$$\begin{aligned}
\frac{\mathrm{d}\boldsymbol{v}}{\mathrm{d}t} &= -\boldsymbol{\nabla}v_k\left(\frac{\partial\nu}{\partial x_k} + \alpha\frac{\partial\chi}{\partial x_k} + \beta\frac{\partial\eta_0}{\partial x_k} + \sigma\frac{\partial s}{\partial x_k}\right) + \boldsymbol{\nabla}\left(\frac{1}{2}\boldsymbol{v}^2 - w\right) + T\boldsymbol{\nabla}s\\
&\quad + \frac{1}{\rho}((\boldsymbol{\nabla}\eta_0\boldsymbol{\cdot}\boldsymbol{J})\boldsymbol{\nabla}\chi - (\boldsymbol{\nabla}\chi\boldsymbol{\cdot}\boldsymbol{J})\boldsymbol{\nabla}\eta_0)\\
&= -\boldsymbol{\nabla}v_k v_k + \boldsymbol{\nabla}\left(\frac{1}{2}\boldsymbol{v}^2 - w\right) + T\boldsymbol{\nabla}s + \frac{1}{\rho}\boldsymbol{J}\times(\boldsymbol{\nabla}\chi\times\boldsymbol{\nabla}\eta_0)\\
&= -\frac{\boldsymbol{\nabla}p}{\rho} + \frac{1}{\rho}\boldsymbol{J}\times\boldsymbol{B}.
\end{aligned} \tag{B3}$$

We have used both (A6) and (A4) in the above derivation. This of course proves that the non-barotropic Euler equations can be derived from the action given in (A1) and hence all the equations of non-barotropic magnetohydrodynamics can be derived from the above action without restricting the variations in any way except on the relevant boundaries and cuts.

REFERENCES

AKHMET'EV, P.M., KUNAKOVSKAYA, O.V. & KUTVITSKII, V.A. 2009 Remark on the dissipation of the magnetic helicity integral. *Theor. Math. Phys.* **158** (1), 125–134.

BARNES, C.W., FERNANDEZ, J.C., HENINS, I., HOIDA, H.W, JARBOE, T.R., KNOX, S.O., MARKLIN, G.J. & MCKENNA, K.F. 1986 Experimental determination of the conservation of magnetic helicity from the balance between source and spheromak. *Phys. Fluids* **29** (10), 3415–3432.

BATCHELOR, G.K. 1967 *An Introduction to Fluid Dynamics*, p. 615. Cambridge University Press.

BISKAMP, D. 1997 *Nonlinear Magnetohydrodynamics*. Cambridge University Press.

BISKAMP, D. 2003 *Magnetohydrodynamic Turbulence*. Cambridge University Press.

BOOZER, A.H. 2005 Physics of magnetically confined plasmas. *Rev. Mod. Phys.* **76** (4), 1071.

BRIARD, A. & GOMEZ, T. 2018 The decay of isotropic magnetohydrodynamics turbulence and the effects of cross-helicity. *J. Plasma Phys.* **84** (1), 905840110.

https://doi.org/10.1017/S002237782300123X Published online by Cambridge University Press

BROWN, M., CANFIELD, R., FIELD, G., KULSRUD, R., PEVTSOV, A., ROSNER, R. & SEEHAFER, N. 1999 Magnetic helicity in space and laboratory plasmas: editorial summary. *Geophys. Monograph-Am. Geophys. Union* **111**, 301–304.

CALKIN, M.G. 1963 An action principle for magnetohydrodynamics. *Can. J. Phys*. **41** (12), 2241–2251.

CANDELARESI, S. & DEL SORDO, F. 2021 Stability of plasmas through magnetic helicity. https://arxiv.org/abs/2112.01193.

CHANDRAN, B.D.G. 2008 Strong anisotropic mhd turbulence with cross helicity. *Astrophys. J*. **685**, 646–658.

CLEBSCH, A. 1857 Uber eine allgemeine transformation der hydro-dynamischen gleichungen. *J. Reine Angew. Math*. **54**, 293–312.

CLEBSCH, A. 1859 Uber die integration der hydrodynamischen gleichungen. *J. Reine Angew. Math*. **56**, 1–10.

FARACO, D. & LINDBERG, S. 2020 Proof of Taylor's conjecture on magnetic helicity conservation. *Commun. Math. Phys*. **373** (2), 707–738.

FREIDBERG, J.P. 1987 *Ideal Magnetohydrodynamics*. Plenum Press.

HAZELTINE, R.D. & MEISS, J.D. 2003 *Plasma Confinement*. Courier Corporation.

HEINONEN, R.A., DIAMOND, P.H., KATZ, M.F.D. & RONIMO, G.E. 2021 On the role of cross-helicity in β-plane magnetohydrodynamic turbulence. https://arxiv.org/abs/2103.08091.

IOVIENO, M., GALLANA, L., FRATERNALE, F., RICHARDSON, J.D., OPHER, M. & TORDELLA, D. 2016 Cross and magnetic helicity in the outer heliosphere from voyager 2 observations. *Eur. J. Mech. (*B*/Fluids)* **55**, 394–401.

KNIZHNIK, K.J., ANTIOCHOS, S.K., KLIMCHUK, J.A. & DEVORE, C.R. 2019 The role of magnetic helicity in coronal heating. *Astrophys. J*. **883** (1), 26.

KUNDU, P.K., COHEN, I.M. & DOWLING, D.R. 2015 *Fluid Mechanics*. Academic.

LANDAU, L.D. & LIFSHITZ, E.M. 1987 Chapter V – thermal conduction in fluids. In *Fluid Mechanics*, 2 edn (ed. L.D. Landau & E.M. Lifshitz), pp. 192–226. Pergamon.

MIZEVA, I.A., STEPANOV, R.A. & FRIK, P.G. 2009 The cross-helicity effect on cascade processes in MHD turbulence. *Doklady Physics* **54** (2), 93–97.

MOBBS, S.D. 1981 Some vorticity theorems and conservation laws for non-barotropic fluids. *J. Fluid Mech*. **108**, 475–483.

MOFFATT, H.K. 1969 The degree of knottedness of tangled vortex lines. *J. Fluid Mech*. **35** (1), 117–129.

MOFFATT, H.K. 1978 *Field Generation in Electrically Conducting Fluids*, vol. 2, p. 5-1. Cambridge University Press.

MOFFATT, H.K. 1992 Relaxation under topological constraints. In *Topological Aspects of the Dynamics of Fluids and Plasmas* (ed. H.K. Moffatt, G.M. Zaslavsky, P. Comte & M. Tabor), pp. 3–28. Springer.

MOFFATT, H.K. & RICCA, R.L. 1995 Helicity and the călugăreanu invariant. In *Knots and Applications* (ed. T.M. Cowan, D. Finkelstein, L.H. Kauffman, E.W. Mielke, H.K. Moffatt, M.G. Rasetti, L. Rozansky & D.W. Walba), pp. 251–269. World Scientific.

OGILVIE, G.I. 2016 Astrophysical fluid dynamics. *J. Plasma Phys*. **82** (3), 205820301.

PEREZ, J.C. & BOLDYREV, S. 2009 Role of cross-helicity in magnetohydrodynamic turbulence. *Phys. Rev. Lett*. **102** (2), 025003.

PRIEST, E. 2014 *Magnetohydrodynamics of the Sun*. Cambridge University Press.

RICCA, R.L. & BERGER, M.A. 1996 Topological ideas and fluid mechanics. *Phys. Today* **49**, 24.

RICCA, R.L. & MOFFATT, H.K. 1992 *Topological Aspects of the of Fluids and Plasmas*. Kluwer.

RUSSELL, A.J.B., YEATES, A.R., HORNIG, G. & WILMOT-SMITH, A.L. 2015 Evolution of field line helicity during magnetic reconnection. *Phys. Plasmas* **22** (3), 032106.

SAKURAI, T. 1979 A new approach to the force-free field and its application to the magnetic field of solar active regions. *Publ. Astron. Soc. Japan* **31**, 209–230.

STURROCK, P.A. 1994 *Plasma Physics: An Introduction to the Theory of Astrophysical, Geophysical and Laboratory Plasmas*. Cambridge University Press.

VERMA, M.K. 2004 Statistical theory of magnetohydrodynamic turbulence: recent results. *Phys. Rep*. **401** (5–6), 229–380.

VERMA, M.K. 2019 *Energy Transfers in Fluid Flows: Multiscale and Spectral Perspectives*. Cambridge University Press.

VERMA, M.K. 2021 Variable energy flux in turbulence. *J. Phys.* A*: Math. Theor*. **55** (1), 013002.

VERMA, M., SHARMA, M., CHATTERJEE, S. & ALAM, S. 2021 Variable energy fluxes and exact relations in magnetohydrodynamics turbulence. *Fluids* **6** (6), 225.

VISHNIAC, E.T. & CHO, J. 2001 Magnetic helicity conservation and astrophysical dynamos. *Astrophys. J.* **550** (2), 752.

WEBB, G.M. & ANCO, S.C. 2017 On magnetohydrodynamic gauge field theory. *J. Phys.* A*: Math. Theor*. **50** (25), 255501.

WEBB, G.M., DASGUPTA, B., MCKENZIE, J.F., HU, Q. & ZANK, G.P. 2014*a* Local and nonlocal advected invariants and helicities in magnetohydrodynamics and gas dynamics I: Lie dragging approach. *J. Phys.* A*: Math. Theor*. **47** (9), 095501.

WEBB, G.M., DASGUPTA, B., MCKENZIE, J.F., HU, Q. & ZANK, G.P. 2014*b* Local and nonlocal advected invariants and helicities in magnetohydrodynamics and gas dynamics: II. Noether's theorems and casimirs. *J. Phys.* A*: Math. Theor*. **47** (9), 095502.

WEBB, G.M. & MACE, R.L. 2015 Potential vorticity in magnetohydrodynamics. *J. Plasma Phys*. **81** (1), 905810115.

WEBB, G., MCKENZIE, J.F. & ZANK, G.P. 2015 Multi-symplectic magnetohydrodynamics: II, addendum and erratum. *J. Plasma Phys*. **81** (6), 905810610.

WOLTJER, L. 1958a On hydromagnetic equilibrium. *Proc. Natl Acad. Sci. USA* **44** (9), 833.

WOLTJER, L. 1958*b* A theorem on force-free magnetic fields. *Proc. Natl Acad. Sci. USA* **44** (6), 489.

YAHALOM, A. 1995 Helicity conservation via the Noether theorem. *J. Math. Phys*. **36** (3), 1324–1327.

YAHALOM, A. 2003 Method and system for numerical simulation of fluid flow. US Patent 6,516,292.

YAHALOM, A. 2013 Aharonov–Bohm effects in magnetohydrodynamics. *Phys. Lett.* A **377** (31–33), 1898–1904.

YAHALOM, A. 2016*a* Non-barotropic magnetohydrodynamics as a five function field theory. *Intl J. Geom. Meth. Mod. Phys*. **13** (10), 1650130.

YAHALOM, A. 2016*b* Simplified variational principles for non-barotropic magnetohydrodynamics. *J. Plasma Phys*. **82**, 905820204.

YAHALOM, A. 2017*a* A conserved local cross helicity for non-barotropic mhd. *Geophys. Astrophys. Fluid Dyn*. **111** (2), 131–137.

YAHALOM, A. 2017*b* Non-barotropic cross-helicity conservation applications in magnetohydrodynamics and the Aharanov–Bohm effect. *Fluid Dyn. Res*. **50** (1), 011406.

YAHALOM, A. 2019 A new diffeomorphism symmetry group of non-barotropic magnetohydrodynamics. *J. Phys.: Conf. Ser.* **1194**, 012113.

YAHALOM, A. & LYNDEN-BELL, D. 2008 Simplified variational principles for barotropic magnetohydrodynamics. *J. Fluid Mech*. **607**, 235.

YAHALOM, A., PINHASI, G.A. & KOPYLENKO, M. 2005 A numerical model based on variational principle for airfoil and wing aerodynamics. 43rd AIAA Aerospace Sciences Meeting and Exhibit, 10–13 January 2005, Reno, Nevada. https://doi.org/10.2514/6.2005-90.

YAHALOM, A. & QIN, H. 2021 Noether currents for Eulerian variational principles in non-barotropic magnetohydrodynamics and topological conservations laws. *J. Fluid Mech*. **908**, A4.

YOKOI, N. 2013 Cross helicity and related dynamo. *Geophys. Astrophys. Fluid Dyn*. **107** (1–2), 114–184.

YOSHIZAWA, A. 1991 Turbulent transport processes in a tokamak's high-mode confinement. *Phys. Fluids* B **3** (10), 2723–2725.

YOSHIZAWA, A. & YOKOI, N. 1993 Turbulent magnetohydrodynamic dynamo for accretion disks using the cross-helicity effect. *Astrophys. J*. **407**, 540–548.

ZANK, G.P., DOSCH, A., HUNANA, P., FLORINSKI, V., MATTHAEUS, W.H. & WEBB, G.M. 2011 The transport of low-frequency turbulence in astrophysical flows. I. Governing equations. *Astrophys. J.* **745** (1), 35.

ZHANG, Y., SHUMLAK, U., NELSON, B.A., GOLINGO, R.P., WEBER, T.R., STEPANOV, A.D., CLAVEAU, E.L., FORBES, E.G., DRAPER, Z.T. & MITRANI, J.M. *et al.* 2019 Sustained neutron production from a sheared-flow stabilized z pinch. *Phys. Rev. Lett*. **122**, 135001.

ZHOU, Y. & MATTHAEUS, W.H. 1990*a* Models of inertial range spectra of interplanetary magnetohydrodynamic turbulence. *J. Geophys. Res.: Space* **95** (A9), 14881–14892.

ZHOU, Y. & MATTHAEUS, W.H. 1990*b* Transport and turbulence modeling of solar wind fluctuations. *J. Geophys. Res.: Space* **95** (A7), 10291–10311.